CMS-SUS-14-006

arXiv:1605.08993v2 [hep-ex] 27 Feb 2017

Search for top squark pair production in compressed-mass-spectrum scenarios in proton-proton collisions at $\sqrt{s} = 8\,\text{TeV}$ using the α_T variable

The CMS Collaboration*

Abstract

An inclusive search is performed for supersymmetry in final states containing jets and an apparent imbalance in transverse momentum, $\vec{p}_\text{T}^{\text{miss}}$, due to the production of unobserved weakly interacting particles in pp collisions at a centre-of-mass energy of 8 TeV. The data, recorded with the CMS detector at the CERN LHC, correspond to an integrated luminosity of $18.5\,\text{fb}^{-1}$. The dimensionless kinematic variable α_T is used to discriminate between events with genuine $\vec{p}_\text{T}^{\text{miss}}$ associated with unobserved particles and spurious values of $\vec{p}_\text{T}^{\text{miss}}$ arising from jet energy mismeasurements. No excess of event yields above the expected standard model backgrounds is observed. The results are interpreted in terms of constraints on the parameter space of several simplified models of supersymmetry that assume the pair production of top squarks. The search provides sensitivity to a broad range of top squark ($\widetilde{\text{t}}$) decay modes, including the two-body decay $\widetilde{\text{t}} \to \text{c}\widetilde{\chi}_1^0$, where c is a charm quark and $\widetilde{\chi}_1^0$ is the lightest neutralino, as well as the four-body decay $\widetilde{\text{t}} \to \text{b}f\bar{f}'\widetilde{\chi}_1^0$, where b is a bottom quark and f and $\bar{f}'$ are fermions produced in the decay of an intermediate off-shell W boson. These modes dominate in scenarios in which the top squark and lightest neutralino are nearly degenerate in mass. For these modes, top squarks with masses as large as 260 and 225 GeV are excluded, respectively, for the two- and four-body decays.

*See Appendix A for the list of collaboration members

1 Introduction

The standard model (SM) is widely regarded as an effective approximation, valid at low energies, of a more complete theory of particle interactions, such as supersymmetry (SUSY) [1–8], which would supersede the SM at higher energy scales. A realisation of SUSY with TeV-scale third-generation squarks is motivated by the cancellation of quadratically divergent loop corrections to the mass of the Higgs boson [9, 10] avoiding the need for significant fine tuning [7, 8, 11]. In R-parity-conserving SUSY [12], supersymmetric particles (sparticles) such as squarks and gluinos are produced in pairs and decay to the lightest stable supersymmetric particle (LSP), which is generally assumed to be a weakly interacting and massive neutralino, $\widetilde{\chi}_1^0$. A characteristic signature of these events is a final state with jets accompanied by an apparent, significant imbalance in transverse momentum, $\vec{p}_\mathrm{T}^{\,\mathrm{miss}}$, due to unobserved $\widetilde{\chi}_1^0$ particles that can carry substantial momentum.

The lack of evidence to date for SUSY at the CERN LHC has led to the careful consideration of regions of the SUSY parameter space that have a relatively weak coverage in the experimental programme. One such class of models is that of compressed mass spectra, in which the LSP lies close in mass to the parent sparticle produced in the collisions. Models in which both the top squark ($\widetilde{\mathrm{t}}$) and neutralino LSP are light and nearly degenerate in mass are phenomenologically well motivated [13–20]. For a mass splitting $\Delta m = m_{\widetilde{\mathrm{t}}} - m_{\widetilde{\chi}_1^0} < m_\mathrm{W}$, where m_W is the mass of the W boson, the decay modes available to the top squark are either loop-induced, flavour-changing neutral current decays to a charm (c) quark and a neutralino, $\widetilde{\mathrm{t}} \to \mathrm{c}\widetilde{\chi}_1^0$, or four-body decays, $\widetilde{\mathrm{t}} \to \mathrm{b}f\bar{f}'\widetilde{\chi}_1^0$, where b is a bottom quark with f and $\bar{f}'$ fermions from, for example, an off-shell W boson decay. Improved experimental acceptance for systems with compressed mass spectra can be achieved by requiring the sparticles to be produced in association with jets from initial-state radiation (ISR). The sparticle decay products from these systems can be Lorentz boosted to values of transverse momentum p_T within the experimental acceptance if they recoil against a sufficiently high-p_T jet from ISR. This topology is exploited by searches that consider "monojet" $+\ \vec{p}_\mathrm{T}^{\,\mathrm{miss}}$ final states [21–23]. The reliance on ISR is reduced for systems with larger Δm, as in this case the sparticle decay products can have sufficiently large values of p_T to lie within the experimental acceptance even without the Lorentz boost from ISR.

This letter presents an inclusive search for the pair production of massive coloured sparticles in final states with two or more energetic jets and $\vec{p}_\mathrm{T}^{\,\mathrm{miss}}$ in pp collisions at $\sqrt{s} = 8\,\mathrm{TeV}$. The data correspond to an integrated luminosity of $18.5 \pm 0.5\,\mathrm{fb}^{-1}$ [24] collected with the CMS detector at the LHC. The search is based upon a kinematic variable α_T, described in Section 3, which offers powerful discrimination against SM multijet production, and adheres to a strategy of maximising experimental acceptance through the application of loose selection requirements to provide sensitivity to a wide range of SUSY models. Previous versions of this search were reported at $\sqrt{s} = 7\,\mathrm{TeV}$ [25–27], and for an initial sample of data corresponding to $11.7\,\mathrm{fb}^{-1}$ at $8\,\mathrm{TeV}$ [28]. Other LHC searches for manifestations of SUSY in all-jet final states are presented in Refs. [21–23, 29–54]. Recent searches for top squark production in leptonic final states can be found in Refs. [55] (and references therein) and [56, 57].

The search makes use of the number of reconstructed jets per event (N_jet), the number of these jets identified as originating from b quarks (N_b), and the sum of the transverse energies of these jets (H_T), where the transverse energy of a jet is given by $E_\mathrm{T} = E \sin\theta$, with E the energy of the jet and θ its polar angle with respect to the beam axis. The three discriminants provide sensitivity to different production mechanisms of massive coloured sparticles at hadron colliders (i.e. squark-squark, squark-gluino, and gluino-gluino), to a large range of mass splittings between the parent sparticle and the LSP, and to third-generation squark signatures. While the

search results can be interpreted with a broad range of models involving the strong production of coloured sparticles leading to final states with both low and high b quark content, we focus on the parameter space of simplified models [58–60] that assumes the pair production of top squarks, including the nearly mass-degenerate scenarios described above. Furthermore, interpretations are provided for top squarks that decay to the $\widetilde{\chi}_1^0$ either directly in association with a top quark ($\widetilde{t} \to t\widetilde{\chi}_1^0$), or via an intermediate lightest chargino $\widetilde{\chi}_1^\pm$ in association with a bottom quark, with the subsequent decay of the $\widetilde{\chi}_1^\pm$ to the $\widetilde{\chi}_1^0$ and a W boson ($\widetilde{t} \to b\widetilde{\chi}_1^\pm \to bW^{\pm(*)}\widetilde{\chi}_1^0$). All models assume only the pair production of the low-mass eigenstate $\widetilde{t}_1$, with the $\widetilde{t}_2$ decoupled to a high mass.

Several aspects of the present search are improved relative to the results of Ref. [28] in order to increase the sensitivity to models with nearly mass-degenerate $\widetilde{t}$ and $\widetilde{\chi}_1^0$ states. The signal region is extended to incorporate events with a low level of jet activity using a parked data set collected with a dedicated trigger stream [61], where "parked" means that, due to limitations in the available processing capability, the data were recorded without being processed through the reconstruction software, and were processed only subsequent to the end of the 2012 data collection period. Furthermore, tight requirements on a combination of kinematic variables are employed to suppress multijet production to the sub-percent level relative to the total remaining number of background events from other SM processes. Finally, an event veto based on isolated tracks is used to further suppress SM background contributions from $\tau \to \text{hadrons} + \nu$ decays and misreconstructed electrons and muons. These features yield an increased experimental acceptance to events with low jet activity, and improvements in the control of SM backgrounds, which are crucial for enhancing sensitivity to new sources of physics with nearly degenerate mass spectra.

2 The CMS detector

The central feature of the CMS detector is a superconducting solenoid providing an axial magnetic field of 3.8 T. The CMS detector is nearly hermetic, which allows for accurate momentum balance measurements in the plane transverse to the beam axis.

Charged particle trajectories are measured by a silicon pixel and strip tracker system, with full azimuthal (ϕ) coverage and a pseudo-rapidity acceptance $|\eta| < 2.5$. Isolated particles of $p_T = 100\,\text{GeV}$ emitted at $|\eta| < 1.4$ have track resolutions of 2.8% in p_T and 10 (30) μm in the transverse (longitudinal) impact parameter [62].

A lead tungstate crystal electromagnetic calorimeter (ECAL) and a brass and scintillator hadron calorimeter (HCAL) surround the tracking volume and provide coverage over $|\eta| < 3.0$. A forward HCAL extends the coverage to $|\eta| < 5.0$. In the barrel section of the ECAL, an energy resolution of about 1% is achieved for unconverted or late-converting photons with energies on the order of several tens of GeV. In the η–ϕ plane, and for $|\eta| < 1.48$, the HCAL cells map onto 5×5 arrays of ECAL crystals to form calorimeter towers projecting radially outwards from a location near the nominal interaction point. At larger values of $|\eta|$, the size of the towers increases and the matching ECAL arrays contain fewer crystals. Within each tower, the energy deposits in ECAL and HCAL cells are summed to define the calorimeter tower energies, subsequently used to provide the energies and directions of reconstructed jets. The HCAL, when combined with the ECAL, measures jet energies with a resolution of approximately 40% at 12 GeV, 5% at 100 GeV, and 4% at 1 TeV.

Muons are identified in gas ionisation detectors embedded in the steel flux-return yoke of the magnet. Muons are measured in the range $|\eta| < 2.4$. By matching track segments recon-

structed in the muon detectors to segments measured in the silicon tracker, a relative transverse momentum resolution of 1.3–2.0% and $<$10% is achieved for muons with, respectively, $20 < p_T < 100$ GeV and $p_T < 1$ TeV [63].

The first level (L1) of the CMS trigger system, composed of custom hardware processors, uses information from the calorimeters and muon detectors to select events of interest within a fixed time interval of less than $4\,\mu$s. The high-level trigger (HLT) processor farm further decreases the event rate from around 100 kHz to about 600 Hz, before data storage. Of these events, about half are reconstructed promptly. The other half represent the parked data set referred to above.

A more detailed description of the CMS detector, together with a definition of the coordinate system used and the relevant kinematic variables, can be found in Ref. [64].

3 The α_T variable

The α_T kinematic variable, first introduced in Refs. [25, 65], is used to efficiently reject events that do not contain significant $\vec{p}_T^{\,\mathrm{miss}}$ or that contain large $\vec{p}_T^{\,\mathrm{miss}}$ only because of transverse momentum mismeasurements, while retaining sensitivity to new-physics events with significant $\vec{p}_T^{\,\mathrm{miss}}$. The α_T variable depends solely on the transverse energies and azimuthal angles of jets, and is intrinsically robust against the presence of jet energy mismeasurements in multijet systems.

For events containing only two jets, α_T is defined as $\alpha_T = E_T^{j_2}/M_T$, where $E_T^{j_2}$ is the transverse energy of the jet with smaller E_T, and M_T is the transverse mass of the dijet system, defined as:

$$M_T = \sqrt{\left(\sum_{i=1}^{2} E_T^{j_i}\right)^2 - \left(\sum_{i=1}^{2} p_x^{j_i}\right)^2 - \left(\sum_{i=1}^{2} p_y^{j_i}\right)^2}, \tag{1}$$

where $E_T^{j_i}$, $p_x^{j_i}$, and $p_y^{j_i}$ are, respectively, the transverse energy and x or y components of the transverse momentum of jet j_i. For a perfectly measured dijet event with $E_T^{j_1} = E_T^{j_2}$ and the jets in the back-to-back configuration ($\Delta\phi = \pi$), and in the limit in which the momentum of each jet is large compared with its mass, the value of α_T is 0.5. For an imbalance in the E_T values of the two back-to-back jets, whether due to an over- or under-measurement of the E_T of either jet, then $E_T^{j_2} < 0.5M_T$. This in turn implies $\alpha_T < 0.5$, giving the variable its intrinsic robustness. Values of α_T significantly greater than 0.5 are observed when the two jets are not back-to-back and recoil against significant, genuine $\vec{p}_T^{\,\mathrm{miss}}$ from weakly interacting particles that escape the detector, such as neutrinos.

The definition of the α_T variable can be generalised for events with more than two jets [25]. The mass scale for any process is characterised through the scalar E_T sum of jets, defined as $H_T = \sum_{i=1}^{N_{\mathrm{jet}}} E_T^{j_i}$, where N_{jet} is the number of jets with E_T above a predefined threshold. The estimator for $|\vec{p}_T^{\,\mathrm{miss}}|$ is given by the magnitude of the vector p_T sum of all the jets, defined by $H_T^{\mathrm{miss}} = |\sum_{i=1}^{N_{\mathrm{jet}}} \vec{p}_T^{\,j_i}|$. For events with three or more jets, a pseudo-dijet system is formed by combining the jets in the event into two pseudo-jets. The total H_T for each of the two pseudo-jets is given by the scalar E_T sum of its contributing jets. The combination chosen is the one that minimises ΔH_T, defined as the difference between the H_T of the two pseudo-jets. This clustering criterion assumes a balanced-momentum hypothesis, $|\vec{p}_T^{\,\mathrm{miss}}| \approx 0$ GeV, which provides the best separation between SM multijet events and events with genuine $\vec{p}_T^{\,\mathrm{miss}}$. The α_T definition can then be generalised to:

$$\alpha_{\mathrm{T}} = \frac{1}{2} \frac{H_{\mathrm{T}} - \Delta H_{\mathrm{T}}}{\sqrt{(H_{\mathrm{T}})^2 - (H_{\mathrm{T}}^{\mathrm{miss}})^2}}. \tag{2}$$

When jet energies are mismeasured, or there are neutrinos from heavy-flavour quark decays, the magnitude of $H_{\mathrm{T}}^{\mathrm{miss}}$ and ΔH_{T} are highly correlated. This correlation is much weaker for R-parity-conserving SUSY events, where each of the two decay chains produces an undetected LSP.

4   Event reconstruction and selection

The event reconstruction and selection criteria described below are discussed in greater detail in Ref. [28]. To suppress SM processes with genuine $\vec{p}_{\mathrm{T}}^{\mathrm{miss}}$ from neutrinos, events containing an isolated electron [66] or muon [63] with $p_{\mathrm{T}} > 10\,\mathrm{GeV}$ are vetoed. Furthermore, events containing an isolated track [67] with $p_{\mathrm{T}} > 10\,\mathrm{GeV}$ are vetoed. Events containing isolated photons [68] with $p_{\mathrm{T}} > 25\,\mathrm{GeV}$ are also vetoed to ensure an event sample comprising only multijet final states.

Jets are reconstructed from the energy deposits in the calorimeter towers, clustered using the anti-k_{T} algorithm [69] with a radius parameter of 0.5. The jet energies measured in the calorimeters are corrected to account for multiple pp interactions within an event (pileup), and to establish a uniform relative response in η and a calibrated absolute response in p_{T} [70]. Jets are identified as originating from b quarks using the "medium" working point of the combined secondary vertex algorithm [71], such that the probability to misidentify jets originating from light-flavour partons (gluons and u, d, or s quarks) as b quark jets is approximately 1% for jets with $p_{\mathrm{T}} = 80\,\mathrm{GeV}$. The "medium" working point results in a b-tagging efficiency, i.e. the probability to correctly identify jets as originating from b quarks, in the range 60–70% depending on the jet p_{T}.

All jets are required to satisfy $|\eta| < 3.0$, and the jet with largest E_{T} is also required to satisfy $|\eta| < 2.5$. All jets and the two jets with largest E_{T} are, respectively, subjected to a nominal ($E_{\mathrm{T}} > 50\,\mathrm{GeV}$) and higher ($E_{\mathrm{T}} > 100\,\mathrm{GeV}$) threshold. Events are required to contain at least two jets that satisfy the aforementioned E_{T} and η requirements. The value of H_{T} for each event is determined from these jets. If $H_{\mathrm{T}} < 375\,\mathrm{GeV}$, the respective jet E_{T} thresholds are lowered to 43 and 87 GeV, H_{T} is recalculated, and the event is reconsidered for selection. If the recalculated H_{T} is less than 325 GeV, the respective E_{T} thresholds are lowered yet further, to 37 and 73 GeV and H_{T} again recalculated. If this newly recalculated H_{T} is less than 200 GeV, the event is rejected. The scheme is summarised in Table 1. Events can be selected with this iterative procedure even if they do not satisfy the sets of tighter requirements on the E_{T} thresholds. The reason why lower jet E_{T} thresholds are employed for $200 < H_{\mathrm{T}} < 375\,\mathrm{GeV}$ is to maintain a similar background composition in all H_{T} bins, and to increase the acceptance for SUSY models characterised by compressed mass spectra. Significant jet activity in the event is established by requiring $H_{\mathrm{T}} > 200\,\mathrm{GeV}$, which also ensures high efficiency for the trigger conditions, described below, used to record the events. Events are vetoed if rare, anomalous signals are identified in the calorimeters [72] or if any jet satisfies $E_{\mathrm{T}} > 50\,\mathrm{GeV}$ and has $|\eta| > 3$, in order to enhance the performance of $H_{\mathrm{T}}^{\mathrm{miss}}$ as an estimator of $|\vec{p}_{\mathrm{T}}^{\mathrm{miss}}|$.

Events are categorised according to the number of jets per event, $2 \leq N_{\mathrm{jet}} \leq 3$ or $N_{\mathrm{jet}} \geq 4$, and the number of reconstructed b quark jets per event, $N_{\mathrm{b}} = 0, 1, 2, 3,$ or ≥ 4. For events containing exactly zero or one b quark jet, we employ eleven bins in H_{T}: three bins at low jet

Table 1: H_T-dependent thresholds on the E_T values of jets and α_T values.

H_T (GeV)	200–275	275–325	325–375	>375
Highest E_T jet (GeV)	73	73	87	100
Next-to-highest E_T jet (GeV)	73	73	87	100
E_T of other jets (GeV)	37	37	43	50
α_T	0.65	0.60	0.55	0.55

activity in the range of $200 < H_T < 375$ GeV, as detailed in Table 1, an additional seven bins 100 GeV wide in the range of $375 < H_T < 1075$ GeV, and an open final bin $H_T > 1075$ GeV. For events containing two or three (at least four) b quark jets, a total of nine (four) bins are used in H_T, with an open final bin $H_T > 875$ (375) GeV. This categorisation according to N_{jet}, N_b, and H_T results in a total of eight (N_{jet}, N_b) event categories and 75 bins. An overview of the binning scheme is provided by Table 3.

For events satisfying the above selection criteria, the multijet background dominates over all other SM sources. Multijet events populate the region $\alpha_T \lesssim 0.5$, and the α_T distribution is characterised by a sharp edge at 0.5, beyond which the multijet event yield falls by several orders of magnitude. Multijet events with extremely rare but large stochastic fluctuations in the calorimetric measurements of jet energies can lead to values of α_T slightly above 0.5. The edge at 0.5 sharpens with increasing H_T for multijet events, primarily due to a corresponding increase in the average jet energy and a consequent improvement in the jet energy resolution. The contribution from multijet events is suppressed by more than five orders of magnitude by imposing the H_T-dependent α_T requirements summarised in Table 1.

Several beam- and detector-related effects, such as interactions from beam halo, reconstruction failures, detector noise, or event misreconstruction due to detector inefficiencies, can lead to events with large, unphysical values of $\vec{p}_T^{miss}$ and values of α_T greater than 0.55. These types of events are rejected with high efficiency by applying a range of vetoes [73].

Two final event vetoes complete the definition of the signal region. An estimator for $\vec{p}_T^{miss}$ is defined by the negative of the vector sum of the transverse momenta of all reconstructed particles in an event, as determined by the particle-flow (PF) algorithm [74, 75]. The magnitude of this vectorial summation is referred to as E_T^{miss}. The first veto concerns the rare circumstance in which several jets, collinear in ϕ and each with p_T below its respective threshold, result in significant H_T^{miss}. This type of background, typical of multijet events, is suppressed while maintaining high efficiency for SM or new-physics processes with genuine $\vec{p}_T^{miss}$ by requiring $H_T^{miss}/E_T^{miss} < 1.25$. The second veto considers the minimum azimuthal separation between a jet and the negative of the vector sum derived from the transverse momenta of all other jets in the event, which is referred to as $\Delta\phi_{min}^*$ [25]. This variable is employed to suppress potential contributions from energetic multijet events that have significant $\vec{p}_T^{miss}$ through the production of neutrinos in semileptonic heavy-flavour decays. Such neutrinos are typically collinear with the axis of a jet. We impose the requirement $\Delta\phi_{min}^* > 0.3$, which effectively suppresses this background as determined using control data.

5   Triggers and data control samples

Candidate signal events are recorded under multiple jet-based trigger conditions that require both H_T and α_T to satisfy predetermined thresholds. The trigger-level jet energies are corrected to account for energy scale and pileup effects. The trigger efficiencies for the SM backgrounds are measured using a sample of $\mu + $ jets events, which provides an unbiased coverage of the

kinematic phase space when the muon is ignored. The efficiencies are determined as a function of N_{jet} and H_T, and lie in the range 79–98% and >99% for $200 < H_T < 375\,\text{GeV}$ and $H_T > 375\,\text{GeV}$, respectively. The inefficiencies at low values of H_T, which are accounted for in the final result, arise from conditions imposed on L1 trigger quantities. Statistical uncertainties of a few percent are considered. Simulation-based studies demonstrate that trigger inefficiencies for signal events are typically negligible.

A set of prescaled H_T trigger conditions is used to record events for a multijet-enriched control sample, defined by relaxed requirements on α_T, $\Delta\phi^*_{min}$, and H_T^{miss}/E_T^{miss} with respect to the signal region. This event sample is used to estimate the multijet background contribution.

Significant background in the signal region is expected from SM processes with genuine $\vec{p}_T^{\,miss}$ in the final state. The dominant processes are the associated production of W or Z bosons and jets, with the decays $Z \to \nu\bar{\nu}$ or $W^\pm \to \ell\nu$ ($\ell = e, \mu, \tau$), and top quark pair production followed by semileptonic top quark decay. Three separate data control regions are used to estimate the background from these processes. The control regions are defined through the selection of $\mu + \text{jets}$, $\mu\mu + \text{jets}$, or $\gamma + \text{jets}$ events [28]. The selection criteria are chosen such that the SM processes and their kinematic properties resemble as closely as possible the SM background behaviour in the signal region, once the muon, dimuon system, or photon are ignored in the determination of quantities such as H_T and α_T. The event selection criteria are defined to ensure that the potential contribution from multijet events or from a wide variety of SUSY models (i.e. so-called signal contamination) is negligible. Events are categorised according to N_{jet}, N_b, and H_T, identically to the scheme used for events in the signal region, as defined in Section 4.

The $\mu + \text{jets}$ sample is recorded using a trigger that requires an isolated muon. The event selection criteria are chosen so that the trigger is maximally efficient ($\approx$90%). Furthermore, the muon is required to be well separated from the jets in the event, and the transverse mass formed by the muon and E_T^{miss} system must lie between 30 and 125 GeV to ensure a sample rich in W bosons (produced promptly or from the decay of top quarks). The $\mu\mu + \text{jets}$ sample uses the same trigger condition (efficiency $\approx$99%) and similar selection criteria as the $\mu + \text{jets}$ sample, specifically requiring two oppositely charged isolated muons that are well separated from the jets in the event, and with a dilepton invariant mass within a $\pm25\,\text{GeV}$ window around the nominal mass of the Z boson. For both the muon and dimuon samples, no requirement is made on α_T, in order to increase the statistical precision of the predictions from these samples. The $\gamma + \text{jets}$ events are recorded using a single-photon trigger condition. The event selection criteria require an isolated photon with $p_T > 165\,\text{GeV}$, $H_T > 375\,\text{GeV}$, and $\alpha_T > 0.55$, yielding a trigger efficiency of $\gtrsim$99%.

6 Multijet background suppression

The signal region is defined in a manner to suppress the expected contribution from multijet events to the sub-percent level relative to the expected background from other SM processes for all event categories and H_T bins. This is achieved through very restrictive requirements on the α_T and $\Delta\phi^*_{min}$ variables, as described above. In this section, we discuss these requirements further, together with the procedure for estimating the remaining multijet background.

Independent estimates are determined per bin in the signal region, defined in terms of N_{jet}, N_b, and H_T. The method utilises the multijet-enriched control sample introduced in Section 5, defined by $0.505 < \alpha_T < 0.55$ and no threshold requirements on $\Delta\phi^*_{min}$ or H_T^{miss}/E_T^{miss}. The event counts in this data sideband are corrected to account for contamination from nonmultijet processes, which are estimated using the method described in Section 7. The method exploits

the evolution of the ratio $\mathcal{R}(\alpha_T)$, defined by the number of (corrected) event counts that satisfy the requirement $H_T^{\mathrm{miss}}/E_T^{\mathrm{miss}} < 1.25$ to the number that fail, as a function of α_T. The ratio $\mathcal{R}(\alpha_T)$ is observed to monotonically fall as a function of α_T and is modelled, independently for each bin, with an exponential function $\mathcal{F}(\alpha_T)$. An additional multijet-enriched data sideband, defined by $H_T^{\mathrm{miss}}/E_T^{\mathrm{miss}} > 1.25$ and $\alpha_T > 0.55$, is used to determine the number of (corrected) events $\mathcal{N}(\alpha_T > \alpha_T^{\mathrm{min}})$ per bin that satisfy a minimum threshold requirement on α_T. Finally, an estimate of the multijet background for each bin is determined as a function of the threshold α_T^{min} based on the product of $\mathcal{N}(\alpha_T > \alpha_T^{\mathrm{min}})$ and the extrapolated value of the ratio from the corresponding fit, $\mathcal{F}(\alpha_T > \alpha_T^{\mathrm{min}})$.

The α_T value required to suppress the predicted multijet contribution to the sub-percent level relative to the total SM background is determined independently for each bin of the signal region. The α_T^{min} thresholds determined from this method are summarised in Table 1 and, for simplicity, are chosen to be identical for all N_{jet} and N_{b} categories. Higher α_T thresholds are required than those used for Ref. [28] because of higher pileup conditions in the latter half of the data collected in 2012 and because of the addition of the low H_T bins.

Various checks are performed in simulation and in data to assure closure, which, in simulation refers to the ability of the method to correctly predict the background rates found in simulated data, and, in data, refers to the consistency between the data-derived predictions for, and counts in, a separate multijet-enriched validation sample in data. The exponential functions are found to adequately model the observed behaviour in data and simulation. Systematic uncertainties in the predictions are obtained from the differences observed using alternative fit functions and can be as large as $\sim$100%.

Following application of the α_T requirements, residual contributions from multijet events with significant $\vec{p}_T^{\mathrm{miss}}$ due to semileptonic heavy-flavour decays are suppressed by requiring $\Delta\phi_{\mathrm{min}}^* > 0.3$, as discussed in Section 4. This suppression is validated in simulation and in data using a control sample defined by the requirements $H_T > 775\,\mathrm{GeV}$ and either $0.51 < \alpha_T < 0.55$ or $H_T^{\mathrm{miss}}/E_T^{\mathrm{miss}} > 1.25$. These events are selected with an unprescaled H_T trigger, allowing a study of the performance of the selection requirements in the low α_T region around 0.51, which corresponds to similar H_T^{miss} values as employed in the lowest H_T bins. From these studies, the remaining multijet background is found to be at the sub-percent level. With this level of suppression, any residual contribution from multijet events is assumed to be negligible compared to the uncertainties associated with the nonmultijet backgrounds (described below) and is ignored.

7 Estimation of nonmultijet backgrounds

In events with few jets or few b quark jets, the largest backgrounds are $Z \rightarrow \nu\bar{\nu} + \mathrm{jets}$ or $W^{\pm} \rightarrow \ell\nu + \mathrm{jets}$. At higher jet or b quark jet multiplicities, $t\bar{t}$ and single top production also become an important source of background. For W boson decays that yield an electron or muon (possibly originating from leptonic τ decays), the background arises when the e or μ is not rejected through the dedicated lepton vetoes. Background also arises when the τ lepton decays to neutrinos and hadrons, which are identified as a jet. The veto of events containing at least one isolated track is efficient at further suppressing these backgrounds, including those from single-prong τ-lepton decays, by as much as $\sim$50% for categories enriched in $t\bar{t}$.

The production of W and Z bosons in association with jets is simulated with the leading-order (LO) MADGRAPH 5.1.1.0 [76] event generator, with up to four additional partons considered in the matrix element calculation. The production of $t\bar{t}$ and single top quark events is generated
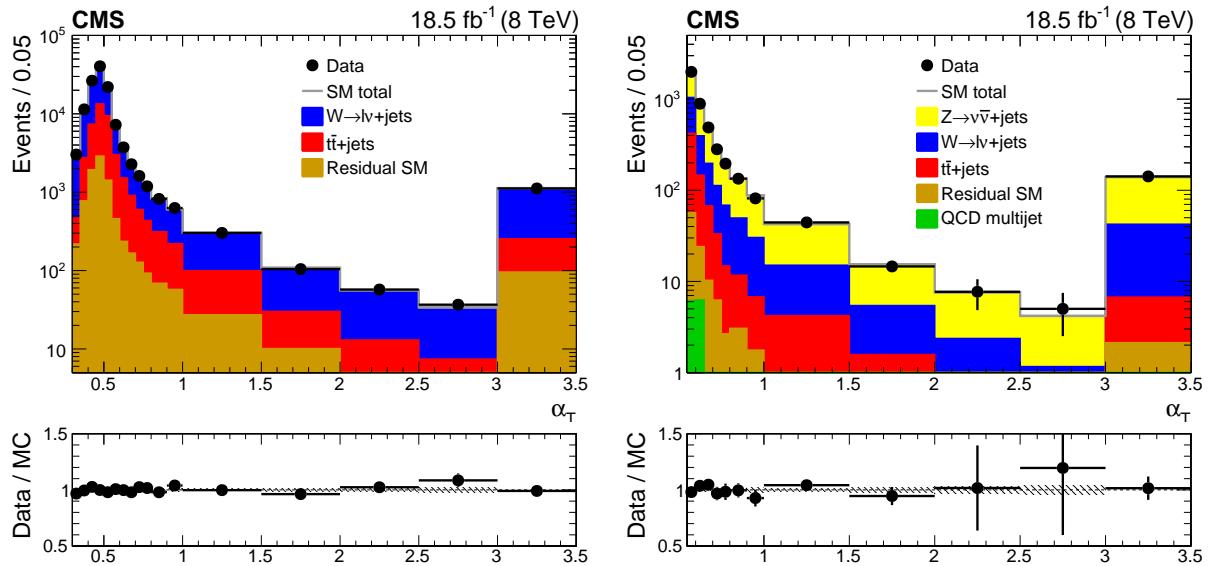
Figure 1: The α_T distribution observed in data for event samples that are recorded with an inclusive set of trigger conditions and satisfy (left) the selection criteria that define the $\mu + $ jets control region or (right) the criteria that define the signal region, with the additional requirement $H_T > 375 \, \text{GeV}$. Event yields observed in data (solid circles) and SM expectations determined from simulation (solid histograms) are shown. Contributions from single top quark, diboson, Drell-Yan, and $t\bar{t} + $ gauge boson production are collectively labelled "Residual SM". The final bin contains the overflow events. The lower panels show the ratios of the binned yields obtained from data and Monte Carlo (MC) simulation as a function of α_T. The statistical uncertainties in the SM expectations are represented by the hatched areas.

with the next-to-leading-order (NLO) POWHEG 1.0 [77–80] program. The LO PYTHIA 6.4.26 [81] program is used to generate WW, WZ, and ZZ (diboson) events, and to describe parton showering and hadronisation for all samples. The CTEQ6L1 [82] and CT10 [83] parton distribution functions (PDFs) are used with MADGRAPH and POWHEG, respectively. The description of the detector response is implemented using the GEANT4 [84] package. The simulated samples are normalised by the most accurate cross section calculations currently available, usually up to next-to-next-to-leading-order (NNLO) accuracy in QCD [85–89]. To model the effects of pileup, the simulated events are generated with a nominal distribution of pp interactions per bunch crossing and then reweighted to match the pileup distribution measured in data.

Figure 1 shows the distributions of the α_T variable obtained from samples of events that satisfy the selection criteria used to define the $\mu + $ jets control region and the signal region. The inclusive requirements $N_{\text{jet}} \geq 2$, $N_b \geq 0$, and $H_T > 200$ and $375 \, \text{GeV}$ for the two samples, respectively, are imposed. The distributions illustrate the background composition of the two samples as determined from simulation. While the figure also demonstrates an adequate modelling of the α_T variable with simulated events, the method employed by the search to estimate the nonmultijet backgrounds is designed to mitigate the effects of simulation mismodelling.

The method relies on the use of transfer factors that are constructed per bin, with a binning scheme defined identically to that of the signal region in terms of N_{jet}, N_b, and H_T, for each control sample in data. The transfer factors are determined using simulated events, and are given by the ratios of the expected yields in the corresponding bins of the signal region and control samples. The transfer factors are used to extrapolate from the event yield measured in a data control sample to the expectation for background from a particular SM process or

processes in the signal region. The method aims to minimise the effects of simulation mis-modelling, as many systematic biases are expected to largely cancel in the ratios used to define the transfer factors. Uncertainties in the transfer factors are determined from a data-derived approach, described below.

The μ + jets data sample provides an estimate of the total contribution from $t\bar{t}$ and W boson production, as well as of the residual contributions from single top quark, diboson, and Drell–Yan ($q\bar{q} \to Z/\gamma^* \to \ell^+\ell^-$) production. Two independent estimates of the background from $Z \to \nu\bar{\nu}$ + jets events with $N_b \leq 1$ are determined, one from the γ + jets data sample and the other from the $\mu\mu$ + jets data sample, which are considered simultaneously in the likelihood function described in Section 8. The γ + jets and $Z \to \mu\mu$ + jets processes have similar kinematic properties when the photon or muons are ignored in the determination of E_T^{miss} and H_T^{miss} [90], although the acceptances differ. An advantage of the γ + jets process is its much larger production cross section compared to the $Z \to \nu\bar{\nu}$ + jets process.

In the case of events with $N_b \geq 2$, the μ + jets sample is also used to estimate the small $Z \to \nu\bar{\nu}$ + jets background because of the limited event counts in the $\mu\mu$ + jets and γ + jets control samples. The method relies on the use of $W \to \mu\nu$ + jets events to predict the $Z \to \nu\bar{\nu}$ + jets background [25, 27, 28]. The method corrects for $t\bar{t}$ contamination in the μ + jets sample, which can be significant in the presence of jets identified as originating from b quarks. However, while the $t\bar{t}$ contamination increases with increasing N_b, the $Z \to \nu\bar{\nu}$ + jets background is reduced to a subdominant level relative to other backgrounds. The method is validated in data control regions defined by samples of events categorised according to N_b. In summary, only the μ + jets sample is used to estimate the total SM background for events with $N_b \geq 2$, whereas all three data control samples are used for events with $N_b \leq 1$.

To maximise sensitivity to new-physics signatures with a large number of b quarks, a method is employed that allows event yields for a given b quark jet multiplicity to be predicted with a higher statistical precision than obtained directly from simulation, particularly for events with a large number of b quark jets ($N_b \geq 2$) [28]. The method relies on generator-level information contained in the simulation to determine the distribution of N_b for a sample of events categorised according to N_{jet} and H_T. First, simulated events are categorised according to the number of jets per event that are matched to underlying b quarks (N_b^{gen}), c quarks (N_c^{gen}), and light-flavoured quarks or gluons (N_q^{gen}). Second, the efficiency ϵ with which b quark jets are identified, and the misidentification probabilities for c quarks and light-flavour partons, f_c and f_q, respectively, are also determined from simulation, with each quantity averaged over jet p_T and η per event category. Corrections to ϵ, f_c, and f_q are applied on a jet-by-jet basis as a function of p_T and η so that they match the corresponding quantity measured in data [71]. Finally, N_b^{tag}, N_c^{tag}, and N_q^{tag} are, respectively, the number of jets identified ("tagged") as originating from b quarks per event when the underlying parton is a b quark, c quark, or a light-flavoured quark or gluon, and $P(N_b^{tag}; N_b^{gen}, \epsilon)$, $P(N_c^{tag}; N_c^{gen}, f_c)$, and $P(N_q^{tag}; N_q^{gen}, f_q)$ are the binomial probabilities for this to happen. These quantities are sufficient to estimate how events are distributed according to N_b per (N_{jet}, H_T) category when summing over all relevant combinations that satisfy the requirements $N_{jet} = N_b^{gen} + N_c^{gen} + N_q^{gen}$ and $N_b = N_b^{tag} + N_c^{tag} + N_q^{tag}$.

The event yields determined with the method described above are subsequently used to determine the transfer factors binned according to N_b (in addition to N_{jet} and H_T). The uncertainties in the transfer factors obtained from simulation are evaluated through sets of closure tests based on events from the data control regions [28]. Each set uses the observed event counts in up to eleven bins in H_T for a given sample of events, along with the corresponding (H_T-dependent) transfer factors obtained from simulation, to determine H_T-dependent predictions

$N_{\mathrm{pred}}(H_{\mathrm{T}})$ for yields in another event sample. The two samples are taken from different data control regions, or are subsets of the same data control sample with differing requirements on N_{jet} or N_{b}. The predictions $N_{\mathrm{pred}}(H_{\mathrm{T}})$ are compared with the H_{T}-binned observed yields $N_{\mathrm{obs}}(H_{\mathrm{T}})$ and the level of closure is defined by the deviation of the ratio $(N_{\mathrm{obs}} - N_{\mathrm{pred}})/N_{\mathrm{pred}}$ from zero. A large number of tests are performed to probe key aspects of the modelling that may introduce an N_{jet}- or H_{T}-dependent source of bias in the transfer factors [28].
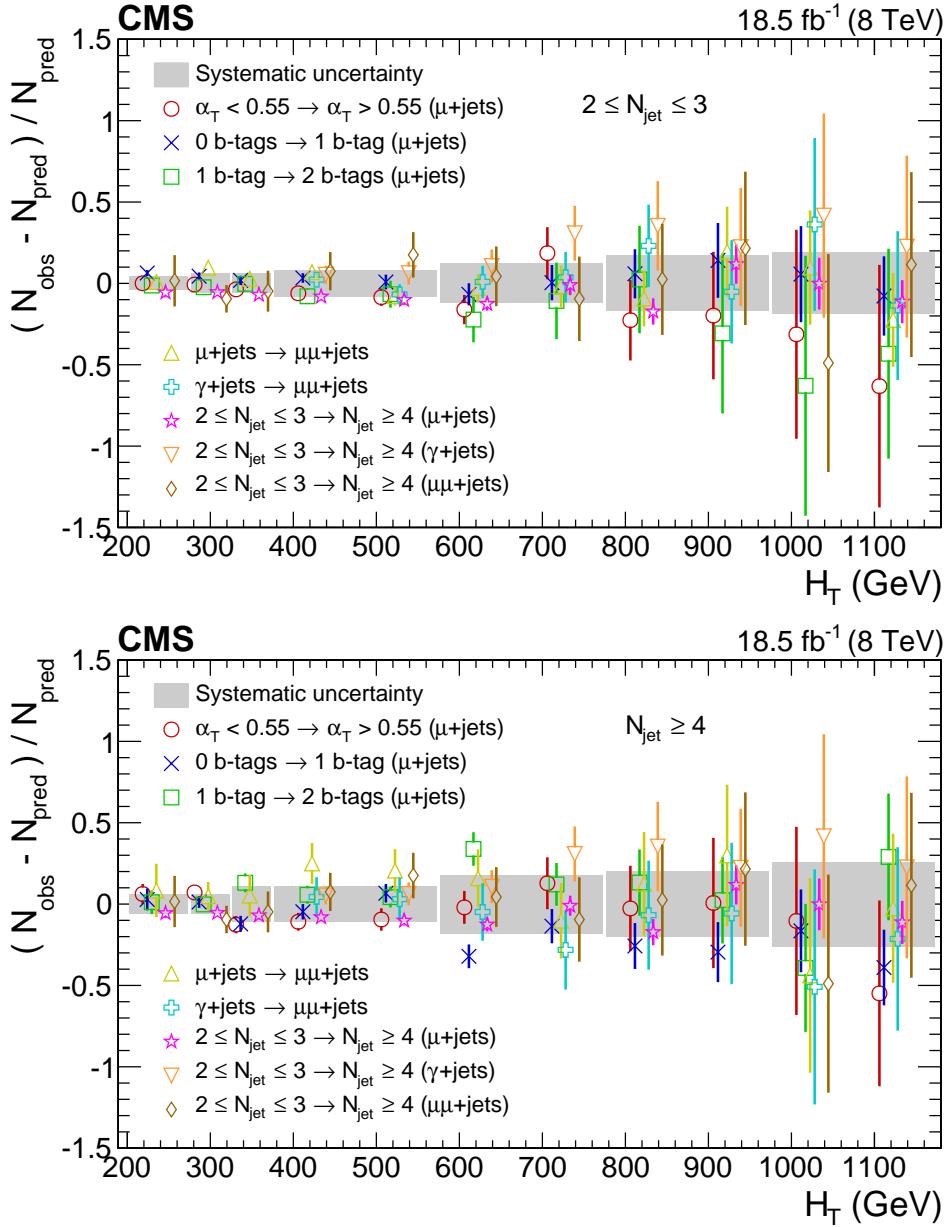
Figure 2: Ratio $(N_{\mathrm{obs}} - N_{\mathrm{pred}})/N_{\mathrm{pred}}$ as a function of H_{T} for different event categories and/or control regions for (upper) events with two or three jets, and (lower) events with four or more jets; "b tag" refers to a reconstructed b quark candidate. Error bars represent statistical uncertainties only, while the grey shaded bands represent the N_{jet}- and H_{T}-dependent uncertainties assumed in the transfer factors, as determined from the procedure described in the text.

Systematic uncertainties are determined from core sets of closure tests, of which the results are shown in Fig. 2. Five sets of tests are performed independently for each of the two N_{jet} categories, and a further three sets that are common to both N_{jet} categories. The tests aim to

probe for the presence of statistically significant biases that could arise due to limitations in the method. For each N_{jet} category, the first three sets of closure tests are performed using the $\mu + \text{jets}$ sample. The first set probes the modelling of the α_{T} distribution for events containing genuine $\vec{p}_{\text{T}}^{\text{miss}}$ from neutrinos (open circle markers). Two sets (crosses, squares) probe the relative composition between $W + \text{jets}$ and top events and the modelling of the reconstruction of b quark jets. The fourth set (triangles) validates the modelling of vector boson production by connecting the $\mu + \text{jets}$ and $\mu\mu + \text{jets}$ control samples, which are enriched in $W + \text{jets}$ and $Z + \text{jets}$ events, respectively. The fifth set (swiss crosses) deals with the consistency between the $\gamma + \text{jets}$ and $\mu\mu + \text{jets}$ samples, which are both used to provide an estimate of the $Z \to \nu\bar{\nu} + \text{jets}$ background. Three further sets of closure tests (stars, inverted triangles, diamonds), one per data control sample, probe the simulation modelling of the N_{jet} distribution for a range of background compositions.

Table 2: Systematic uncertainties (%) in the transfer factors, in intervals of N_{jet} and H_{T}.

	H_{T} region (GeV)						
N_{jet}	200–275	275–325	325–375	375–575	575–775	775-975	> 975
2–3	4	6	6	8	12	17	19
≥ 4	6	6	11	11	18	20	26

The closure tests reveal no significant biases or dependency on N_{jet} nor H_{T}. Systematic uncertainties in the transfer factors are determined from the variance in $(N_{\text{obs}} - N_{\text{pred}})/N_{\text{pred}}$, weighted to account for statistical uncertainties, for all closure tests within an individual H_{T} bin in the range $200 < H_{\text{T}} < 375\,\text{GeV}$ and for each N_{jet} category. For the region $H_{\text{T}} > 375\,\text{GeV}$, all tests within $200\,\text{GeV}$-wide intervals in H_{T}, defined by pairs of adjacent bins, are combined to determine the systematic uncertainty, which is assumed to be fully correlated for bins within each interval, and fully uncorrelated for different H_{T} intervals and N_{jet} categories. The magnitudes of the systematic uncertainties are indicated by shaded grey bands in Fig. 2 and summarised in Table 2. The same (uncorrelated) value of systematic uncertainty is assumed for each N_{b} category. An independent study is performed to assess the effect of uncertainties in the simulation modelling of the efficiency and misidentification rates for jets originating from b quarks and from light-flavoured quarks or gluons. These uncertainties are found to be at the sub-percent level, subdominant relative to the values in Table 2, and therefore considered to be negligible.

8 Results and interpretation

For a given category of events satisfying requirements on both N_{jet} and N_{b}, a likelihood model of the observations in all data samples is used to obtain a consistent prediction of the SM backgrounds and to test for the presence of a variety of signal models. This is written as:

$$
\begin{aligned}
L_{N_{\text{jet}}, N_{\text{b}}} &= L_{\text{SR}} L_{\mu} L_{\mu\mu} L_{\gamma}, \quad (0 \leq N_{\text{b}} \leq 1) \\
L_{N_{\text{jet}}, N_{\text{b}}} &= L_{\text{SR}} L_{\mu}, \quad\quad\quad\quad (N_{\text{b}} \geq 2)
\end{aligned}
\tag{3}
$$

where $L_{\text{SR}} = \prod_i \text{Pois}(n^i \mid b^i + s^i)$ is a likelihood function comprising a product of Poisson terms that describe the yields in each of the H_{T} bins of the signal region for given values of N_{jet} and N_{b}. In each bin of H_{T} (index i), the observation n^i is modelled as a Poisson variable distributed about the sum of the SM expectation b^i and a potential contribution from a signal model s^i (assumed to be zero in the following discussion). The contribution from multijet production is assumed to be zero, based on the studies described in Section 6. The SM expectations in the

Table 3: Observed event yields in data and the "a priori" SM expectations determined from event counts in the data control samples and transfer factors from simulation, in bins of H_T, and categorised according to N_{jet} and N_b. Also shown are the SM expectations (labelled "SM") obtained from a combined fit to control and signal regions under the SM hypothesis. The quoted uncertainties include the statistical as well as systematic components. For each row that lists fewer than the full set of columns, the final entry represents values obtained for an open final H_T bin.

Category		H_T (GeV)										
(N_{jet}, N_b)		200–275	275–325	325–375	375–475	475–575	575–675	675–775	775–875	875–975	975–1075	1075–∞
$(2–3,0)$	Data	13090	5331	3354	2326	671	206	76	29	10	9	2
$(2–3,0)$	a priori	12410^{+370}_{-410}	5540^{+340}_{-230}	3330^{+130}_{-170}	2400^{+120}_{-90}	663^{+34}_{-26}	225^{+21}_{-17}	$68.5^{+6.9}_{-6.7}$	$26.5^{+3.9}_{-3.0}$	$10.3^{+1.9}_{-2.1}$	$5.1^{+1.0}_{-1.1}$	$4.5^{+0.9}_{-0.9}$
$(2–3,0)$	SM	13030^{+90}_{-120}	5348^{+85}_{-67}	3351^{+56}_{-50}	2351^{+38}_{-45}	655^{+14}_{-11}	218^{+12}_{-17}	$68.5^{+4.9}_{-4.8}$	$27.2^{+3.0}_{-3.0}$	$10.4^{+1.5}_{-1.6}$	$5.6^{+1.0}_{-1.0}$	$4.3^{+0.7}_{-1.0}$
$(2–3,1)$	Data	1733	833	527	356	90	31	6	4	1	0	1
$(2–3,1)$	a priori	1669^{+65}_{-67}	853^{+50}_{-46}	525^{+37}_{-24}	391^{+23}_{-21}	$94.3^{+6.0}_{-5.6}$	$24.5^{+2.5}_{-3.6}$	$9.0^{+1.2}_{-1.4}$	$2.8^{+0.6}_{-0.8}$	$2.5^{+0.8}_{-0.9}$	$0.3^{+0.2}_{-0.1}$	$0.2^{+0.1}_{-0.1}$
$(2–3,1)$	SM	1711^{+37}_{-33}	839^{+21}_{-25}	526^{+20}_{-17}	372^{+12}_{-14}	$90.6^{+5.1}_{-4.6}$	$25.8^{+2.9}_{-2.6}$	$8.7^{+0.8}_{-1.4}$	$3.0^{+0.7}_{-0.6}$	$2.2^{+0.8}_{-0.6}$	$0.3^{+0.2}_{-0.1}$	$0.2^{+0.1}_{-0.2}$
$(2–3,2)$	Data	172	116	101	55	16	9	0	0	0		
$(2–3,2)$	a priori	187^{+7}_{-8}	118^{+7}_{-7}	$98.7^{+7.1}_{-7.0}$	$61.3^{+5.9}_{-5.5}$	$12.3^{+1.7}_{-1.0}$	$2.8^{+0.5}_{-0.6}$	$0.7^{+0.2}_{-0.2}$	$0.2^{+0.1}_{-0.1}$	<0.1		
$(2–3,2)$	SM	184^{+5}_{-7}	117^{+7}_{-5}	$99.4^{+5.4}_{-4.6}$	$60.2^{+3.5}_{-3.8}$	$12.4^{+1.2}_{-1.0}$	$3.3^{+0.6}_{-0.5}$	$0.7^{+0.2}_{-0.2}$	$0.2^{+0.1}_{-0.1}$	<0.1		
$(\geq 4,0)$	Data	99	568	408	336	211	117	38	13	9	4	6
$(\geq 4,0)$	a priori	108^{+10}_{-12}	497^{+34}_{-36}	403^{+36}_{-33}	327^{+25}_{-22}	193^{+14}_{-13}	95^{+13}_{-11}	$40.3^{+5.9}_{-4.4}$	$14.5^{+3.5}_{-2.4}$	$7.1^{+1.7}_{-1.4}$	$3.2^{+0.7}_{-1.0}$	$2.9^{+0.7}_{-0.5}$
$(\geq 4,0)$	SM	104^{+6}_{-8}	544^{+21}_{-18}	407^{+18}_{-18}	337^{+15}_{-10}	202^{+10}_{-8}	105^{+9}_{-7}	$42.5^{+4.5}_{-3.3}$	$14.3^{+1.7}_{-2.5}$	$7.5^{+1.4}_{-1.5}$	$3.5^{+0.8}_{-0.8}$	$3.4^{+1.0}_{-0.7}$
$(\geq 4,1)$	Data	38	195	210	159	83	33	7	10	4	1	1
$(\geq 4,1)$	a priori	$39.2^{+3.0}_{-3.5}$	215^{+12}_{-16}	208^{+24}_{-22}	150^{+15}_{-11}	$75.8^{+7.8}_{-6.6}$	$28.6^{+3.8}_{-3.7}$	$10.3^{+2.1}_{-1.4}$	$5.1^{+1.3}_{-0.9}$	$2.0^{+0.7}_{-0.5}$	$0.8^{+0.4}_{-0.3}$	$0.9^{+0.6}_{-0.4}$
$(\geq 4,1)$	SM	$38.9^{+2.2}_{-3.7}$	206^{+12}_{-10}	209^{+13}_{-10}	157^{+9}_{-9}	$79.3^{+5.2}_{-4.7}$	$29.4^{+3.8}_{-2.2}$	$9.9^{+1.9}_{-1.3}$	$6.2^{+1.2}_{-1.1}$	$2.3^{+0.7}_{-0.7}$	$0.9^{+0.3}_{-0.3}$	$0.9^{+0.3}_{-0.4}$
$(\geq 4,2)$	Data	16	81	88	64	43	14	5	1	1		
$(\geq 4,2)$	a priori	$12.3^{+1.0}_{-1.0}$	$76.7^{+5.6}_{-5.2}$	93^{+11}_{-9}	$63.0^{+7.8}_{-5.7}$	$34.0^{+3.6}_{-3.4}$	$10.1^{+2.6}_{-1.8}$	$3.4^{+0.9}_{-0.6}$	$1.0^{+0.2}_{-0.2}$	$0.7^{+0.1}_{-0.2}$		
$(\geq 4,2)$	SM	$12.5^{+1.0}_{-1.0}$	$77.8^{+4.7}_{-4.6}$	$90.2^{+9.0}_{-6.5}$	$66.1^{+4.6}_{-4.8}$	$36.3^{+3.4}_{-2.9}$	$11.4^{+1.8}_{-1.9}$	$3.9^{+0.8}_{-0.7}$	$1.0^{+0.2}_{-0.3}$	$0.7^{+0.1}_{-0.2}$		
$(\geq 4,3)$	Data	0	7	5	5	6	1	1	0	0		
$(\geq 4,3)$	a priori	$1.1^{+0.2}_{-0.1}$	$8.2^{+0.6}_{-0.9}$	$11.1^{+2.0}_{-1.6}$	$7.4^{+1.1}_{-1.0}$	$4.0^{+0.5}_{-0.6}$	$1.1^{+0.3}_{-0.3}$	$0.4^{+0.2}_{-0.1}$	$0.1^{+0.1}_{-0.0}$	<0.1		
$(\geq 4,3)$	SM	$1.1^{+0.2}_{-0.2}$	$8.1^{+0.9}_{-0.9}$	$9.9^{+1.5}_{-1.3}$	$7.2^{+0.9}_{-0.7}$	$4.1^{+0.6}_{-0.6}$	$1.1^{+0.3}_{-0.3}$	$0.4^{+0.1}_{-0.1}$	$0.1^{+0.1}_{-0.0}$	<0.1		
$(\geq 4,\geq 4)$	Data	0	0	0	2							
$(\geq 4,\geq 4)$	a priori	<0.1	$0.2^{+0.1}_{-0.1}$	$0.5^{+0.3}_{-0.3}$	$0.3^{+0.2}_{-0.2}$							
$(\geq 4,\geq 4)$	SM	<0.1	$0.1^{+0.1}_{-0.1}$	$0.4^{+0.2}_{-0.3}$	$0.4^{+0.2}_{-0.2}$							

signal region are related to the expected yields in the $\mu + $ jets, $\mu\mu + $ jets, and $\gamma + $ jets control samples via the transfer factors derived from simulation. Analogous to L_{SR}, the likelihood functions L_μ, $L_{\mu\mu}$, and L_γ describe the yields in the H_T bins of the $\mu + $ jets, $\mu\mu + $ jets, and $\gamma + $ jets control samples for the same values of N_{jet} and N_b as the signal region. For the category of events with $N_b \geq 2$, only the $\mu + $ jets control sample is used in the likelihood to determine the total contribution from all nonmultijet SM backgrounds in the signal region. The systematic uncertainties in the transfer factors, determined from the ensemble of closure tests described above and with magnitudes in the range 4–26% (Table 2), are accommodated in the likelihood function through a nuisance parameter associated with each transfer factor used in the background estimation for each (N_{jet}, N_b) category and H_T interval. The H_T intervals are defined by pairs of adjacent H_T bins for the region $H_T > 375$ GeV, as described in Section 7, and so adjacent bins share the same nuisance parameter. The measurements of these parameters are assumed to follow a lognormal distribution.

Table 3 summarises the observed event yields and expected number of events from SM pro-

cesses in the signal region as a function of N_{jet}, N_{b}, and H_{T}. The "a priori" SM expectations are determined from event counts in the data control samples and transfer factors from simulation, and are therefore independent of the signal region. No significant discrepancies are observed between the "a priori" SM expectations and the observed event yields. In addition, a simultaneous fit to data in the signal region and in up to three control regions is performed. The likelihood function is maximised over all fit parameters under the SM-only hypothesis in order to estimate the yields from SM processes in each bin in all regions, in the absence of an assumed contribution from signal events. Table 3 summarises these estimates (labelled "SM") for the signal region. A goodness-of-fit test is performed to quantify the degree of compatibility between the observed yields and the expectations under the background-only hypothesis. The test is based on a log likelihood ratio and the alternative hypothesis is defined by a "saturated" model [91]. The p-value probabilities for all N_{jet} and N_{b} categories are found to be uniformly distributed, with a minimum value of 0.19.

The results of this search are interpreted in terms of limits on the parent sparticle and LSP masses in the parameter space of simplified models [58–60] that represent the direct pair production of top squarks and the decay modes $\widetilde{t} \to c\widetilde{\chi}_1^0$, $\widetilde{t} \to bf\bar{f}'\widetilde{\chi}_1^0$, $\widetilde{t} \to b\widetilde{\chi}_1^\pm$ followed by $\widetilde{\chi}_1^\pm \to W^\pm\widetilde{\chi}_1^0$, and $\widetilde{t} \to t\widetilde{\chi}_1^0$. The CL_s method [92, 93] is used to determine upper limits at the 95% confidence level (CL) on the production cross section of a signal model, using the one-sided (LHC-style) profile likelihood ratio as the test statistic [94]. The sampling distributions for the test statistic are generated from pseudo-experiments using the respective maximum likelihood values of nuisance parameters determined from a simultaneous fit to the pseudo-data, in the 75 bins of the signal region and in the corresponding bins of up to three control samples, under the SM background-only and signal + background hypotheses. The potential contributions of signal events to each of the signal and control samples are considered, but the only significant contribution occurs in the signal region and not the control samples.

The event samples for the simplified models are generated with the LO MADGRAPH 5.1.1.0 generator, which considers up to two additional partons in the matrix element calculation. Inclusive, process-dependent, NLO calculations of SUSY production cross sections, with next-to-leading-logarithmic (NLL) corrections, are obtained with the program PROSPINO 2.1 [95–100]. All events are generated using the CTEQ6L1 PDFs. As for SM processes, the simulated events are generated with a nominal pileup distribution and then reweighted to match the distribution observed in data. The detector response is provided by the CMS fast simulation package [101].

Experimental uncertainties in the expected signal yields are considered. Contributions to the overall systematic uncertainty arise from various sources such as the uncertainties from the choice of PDFs, the jet energy scale, the modelling of the efficiency and misidentification probability of b quark jets in simulation, the integrated luminosity [24], and various event selection criteria. The magnitude of each contribution depends on the model, the masses of the parent sparticle and LSP, and the event category under consideration. Uncertainties in the jet energy scale are typically dominant ($\sim$15%) for models with mass splittings that satisfy $\Delta m > m_{\text{t}}$, where m_{t} is the top quark mass. The acceptance for models with mass splittings satisfying $\Delta m < m_{\text{t}}$ is due in large part to ISR, the modelling of which contributes the dominant systematic uncertainty for systems with a compressed mass spectrum. An uncertainty of $\sim$20% is determined by comparing the simulated and measured p_{T} spectra of the system recoiling against the ISR jets in $t\bar{t}$ events, using the technique described in Ref. [67]. For the aforementioned simplified models, the effect of uncertainties in the distribution of signal events is generally small compared with the uncertainties in the experimental acceptance. The total systematic uncertainty in the yield of signal is found to be in the range 5–36%, depending on N_{jet} and N_{b},

and is taken into account through a nuisance parameter that follows a lognormal distribution.

Figure 3 shows the observed upper limit on the production cross section at 95% confidence level (CL), as a function of the top squark and $\widetilde{\chi}_1^0$ masses, for a range of simplified models based on the pair production of top squarks, together with excluded mass regions.

Figures 3 (upper left and right) show the sensitivity of this analysis to the decay modes $\widetilde{t} \to c\widetilde{\chi}_1^0$ and $\widetilde{t} \to bf\bar{f}'\widetilde{\chi}_1^0$, respectively. Models with Δm as small as 10 GeV are considered, and the top squarks are assumed to decay promptly. The excluded regions are determined using the NLO+NLL cross sections for top squark pair production, assuming that b squarks, light-flavoured squarks, and gluinos are too heavy to be produced in the pp collisions. Also shown are the excluded regions observed when the production cross section is changed by its theoretical uncertainty, and the expected region of exclusion, as well as those determined for both ± 1 and ± 2 standard deviation (σ) changes in experimental uncertainties. The range of excluded top squark masses is sensitive to both the decay mode and Δm. For the decay $\widetilde{t} \to c\widetilde{\chi}_1^0$, the expected excluded region is relatively stable as a function of Δm, with $\widetilde{t}$ masses below 285 and 325 GeV excluded, respectively, for $\Delta m = 10$ and 80 GeV. The observed exclusion, assuming the theoretical production cross section reduced by its 1σ uncertainty, is weaker, with $\widetilde{t}$ masses below 240 and 260 GeV excluded for $\Delta m = 10$ and 80 GeV. For the decay $\widetilde{t} \to bf\bar{f}'\widetilde{\chi}_1^0$, the expected excluded mass region is strongly dependent on Δm, weakening considerably for increasing values of Δm due to the increased momentum phase space available to leptons produced in the four-body decay. Top squark masses below 265 and 165 GeV are excluded based on the expected results, respectively, for $\Delta m = 10$ and 80 GeV. The observed exclusion is again weaker, with masses below 225 and 130 GeV excluded. The nonsmooth behaviour of the exclusion contours is the result of statistical fluctuations and the sparseness of the scan over the mass parameter space, and does not represent a kinematical effect.

Figures 3 (middle left and right) show the limits on the allowed cross section for the decay $\widetilde{t} \to b\widetilde{\chi}_1^\pm$, followed by a decay of the $\widetilde{\chi}_1^\pm$ to the $\widetilde{\chi}_1^0$ and to either an on- or off-shell W boson, depending on the mass difference between the $\widetilde{\chi}_1^\pm$ and $\widetilde{\chi}_1^0$. For a model with $m_{\widetilde{\chi}_1^\pm} = 0.25 m_{\widetilde{t}} + 0.75 m_{\widetilde{\chi}_1^0}$, shown in Fig. 3 (middle left), the analysis has sensitivity in the region $m_{\widetilde{\chi}_1^\pm} - m_{\widetilde{\chi}_1^0} < m_W$, excluding $\widetilde{\chi}_1^0$ masses up to 225 GeV and $\widetilde{t}$ masses up to 350 GeV. Models that satisfy $m_{\widetilde{\chi}_1^\pm} < 91.9$ GeV, or $m_{\widetilde{\chi}_1^\pm} < 103.5$ GeV and $m_{\widetilde{\chi}_1^\pm} - m_{\widetilde{\chi}_1^0} < 5$ GeV, are already excluded by a combination of results obtained from the ALEPH, DELPHI, L3, and OPAL experiments at LEP [102, 103]. For a model with $m_{\widetilde{\chi}_1^\pm} = 0.75 m_{\widetilde{t}} + 0.25 m_{\widetilde{\chi}_1^0}$, shown in Fig. 3 (middle right), $\widetilde{t}$ masses up to 400 GeV can be excluded but the reach in $\widetilde{\chi}_1^0$ mass is reduced.

Figure 3 (lower left) shows the results of the analysis for the decay $\widetilde{t} \to t\widetilde{\chi}_1^0$. Both two- and three-body decays are considered, for which the latter scenario involves an off-shell top quark. The polarizations of the top quarks are model dependent and are non-trivial functions of the top-squark and neutralino mixing matrices [104]. Simulated events of the production and decay of top squark pairs are generated without polarization of the top quarks. Models with $m_{\widetilde{t}} < 200$ GeV are not considered, due to significant signal contributions in the control regions. Top squark masses up to 500 GeV are excluded, and $\widetilde{\chi}_1^0$ masses up to 100 and 50 GeV are excluded for the two- and three-body decays, respectively. As in Fig. 3 (middle right), the observed limit is around 2σ below the expected result for large values of $m_{\widetilde{t}}$. This is mainly due to an excess of observed counts in data in the $N_b = 2$ categories in the region of $500 < H_T < 700$ GeV, which is compatible with a statistical fluctuation. The observed limits lie closer to the expected values at low top squark masses, which correspond to lower values of H_T for which good agreement between the data and SM background predictions is observed.
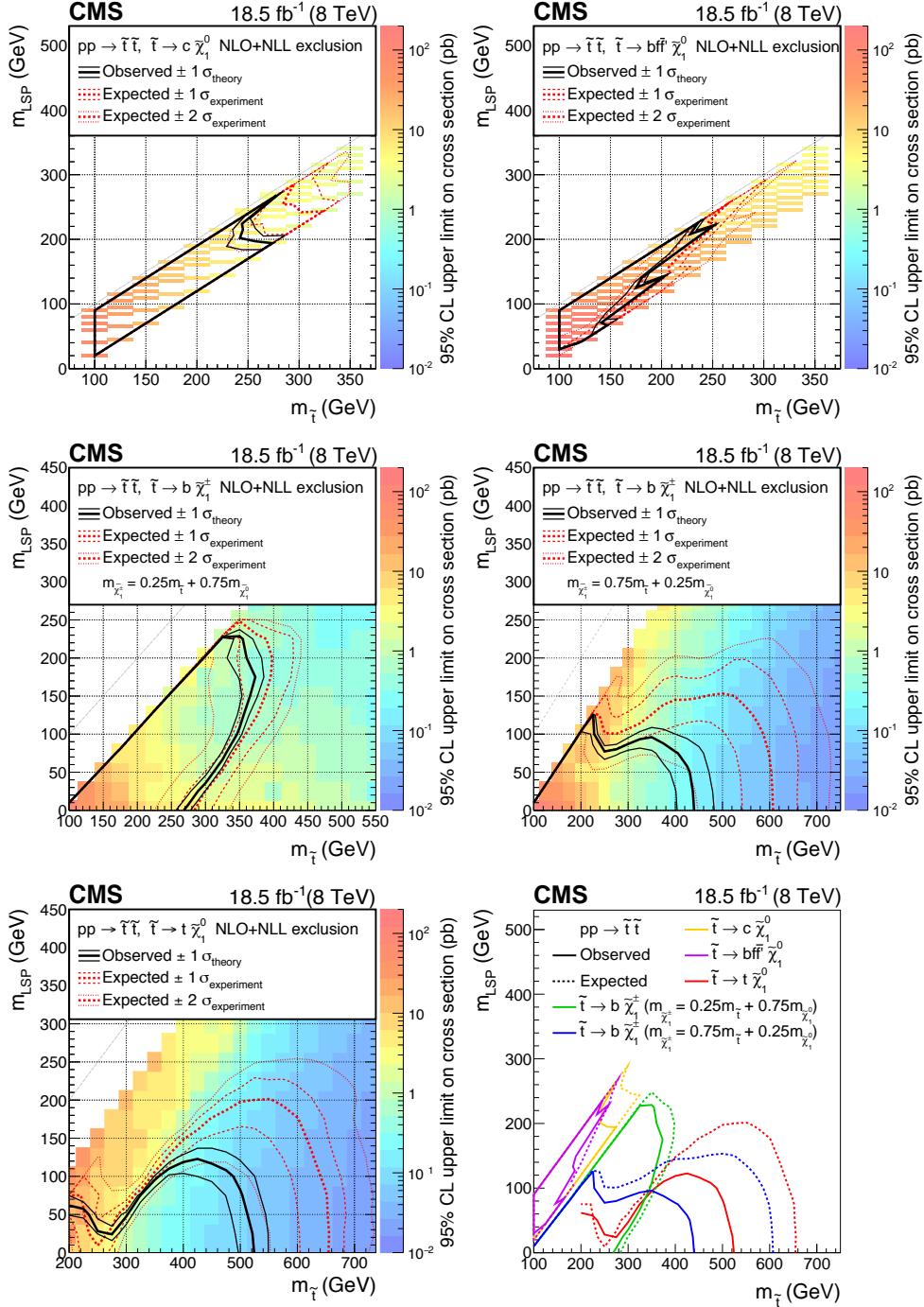
Figure 3: Observed upper limits on the production cross section at 95% CL (indicated by the colour scale) as a function of the top squark and $\widetilde{\chi}_1^0$ masses for (upper left) $\widetilde{t} \to c\widetilde{\chi}_1^0$, (upper right) $\widetilde{t} \to bf\bar{f}'\widetilde{\chi}_1^0$, (middle left) $\widetilde{t} \to b\widetilde{\chi}_1^\pm$ with $m_{\widetilde{\chi}_1^\pm} = 0.25m_{\widetilde{t}} + 0.75m_{\widetilde{\chi}_1^0}$, (middle right) $\widetilde{t} \to b\widetilde{\chi}_1^\pm$ with $m_{\widetilde{\chi}_1^\pm} = 0.75m_{\widetilde{t}} + 0.25m_{\widetilde{\chi}_1^0}$, and (lower left) $\widetilde{t} \to t\widetilde{\chi}_1^0$. The black solid thick curves indicate the observed exclusion assuming the NLO+NLL SUSY production cross sections; the thin black curves show corresponding $\pm1\sigma$ theoretical uncertainties. The red thick dashed curves indicate median expected exclusions and the thin dashed and dotted curves indicate, respectively, their $\pm1\sigma$ and $\pm2\sigma$ experimental uncertainties. A summary of the observed (solid) and median expected (dotted) exclusion contours is presented (lower right). The grey dotted diagonal lines delimit the region for which $m_{\widetilde{t}} > m_{\widetilde{\chi}_1^0}$. (For interpretation of the references to colour in this figure legend, the reader is referred to the web version of this article.)

Figure 3 (lower right) presents a summary of all the expected and observed exclusion contours and indicates that the analysis has good sensitivity across many different decay signatures in the $m_{\tilde{t}}$–$m_{\tilde{\chi}_1^0}$ plane. The sensitivity for these models is typically driven by categories involving events satisfying $N_{\text{jet}} \geq 4$ and $1 \leq N_{\text{b}} \leq 2$, while events with lower N_{jet} and N_{b} multiplicities become increasingly important for nearly mass-degenerate models.

9 Summary

An inclusive search for supersymmetry with the CMS detector is reported, based on data from pp collisions collected at $\sqrt{s} = 8\,\text{TeV}$, corresponding to an integrated luminosity of $18.5 \pm 0.5\,\text{fb}^{-1}$. The final states analysed contain two or more jets with large transverse energies and a significant imbalance in the event transverse momentum, as expected in the production and decay of massive squarks and gluinos. Dedicated triggers made it possible to extend the phase space covered in this search to values of H_{T} and $H_{\text{T}}^{\text{miss}}$ as low as 200 and 130 GeV, respectively. These regions of low H_{T} and $H_{\text{T}}^{\text{miss}}$ correspond to regions of phase space that are highly populated in models with low-mass squarks and nearly degenerate mass spectra. The signal region is binned according to H_{T}, the number of reconstructed jets, and the number of jets identified as originating from b quarks. The sum of standard model backgrounds in each bin is estimated from a simultaneous binned likelihood fit to the event yields in the signal region and in $\mu + \text{jets}$, $\mu\mu + \text{jets}$, and $\gamma + \text{jets}$ control samples. The observed yields in the signal region are found to be in agreement with the expected contributions from standard model processes.

Limits are determined in the mass parameter space of simplified models that assume the direct pair production of top squarks. A comprehensive study of top squark decay modes is performed and interpreted in the parameter space of the loop-induced two-body decays to the neutralino and one c quark ($\tilde{t} \to c\tilde{\chi}_1^0$); four-body decays to the neutralino, one b quark, and an off-shell W boson ($\tilde{t} \to bf\bar{f}'\tilde{\chi}_1^0$); decays to one b quark and the lightest chargino ($\tilde{t} \to b\tilde{\chi}_1^\pm$), followed by the decay of the chargino to the lightest neutralino and an (off-shell) W boson; and the decay to a top quark and neutralino ($\tilde{t} \to t\tilde{\chi}_1^0$). In the region $m_{\tilde{t}} - m_{\tilde{\chi}_1^0} < m_{\text{W}}$, top squarks with masses as large as 260 and 225 GeV, and neutralino masses up to 240 and 215 GeV, are excluded, respectively, for the two- and four-body decay modes. For top squark decays to $b\tilde{\chi}_1^\pm$, top squark masses up to 400 GeV and neutralino masses up to 225 GeV are excluded, depending on the mass of the chargino. For top squarks decaying to a top quark and a neutralino, top squark masses up to 500 GeV and neutralino masses up to 105 GeV are excluded.

In summary, the analysis provides sensitivity across a large region of parameter space in the $(m_{\tilde{t}}, m_{\tilde{\chi}_1^0})$ plane, covering several relevant top squark decay modes. In particular, the application of low thresholds to maximise signal acceptance provides sensitivity to models with compressed mass spectra. For top squark decays to $b\tilde{\chi}_1^\pm$, where the W boson from the $\tilde{\chi}_1^\pm$ decay is off-shell, the presented studies improve on existing limits. Mass exclusions are reported in previously unexplored regions of the $(m_{\tilde{t}}, m_{\tilde{\chi}_1^\pm}, m_{\tilde{\chi}_1^0})$ parameter space that satisfy $100\,\text{GeV} < \Delta m < m_{\text{t}}$, of up to $m_{\tilde{t}} = 325$, $m_{\tilde{\chi}_1^\pm} = 250$, and $m_{\tilde{\chi}_1^0} = 225\,\text{GeV}$. For the region $\Delta m < m_{\text{W}}$, the search provides the strongest expected mass exclusions, up to $m_{\tilde{t}} = 325\,\text{GeV}$, for the two-body decay $\tilde{t} \to c\tilde{\chi}_1^0$ when $30\,\text{GeV} < \Delta m < m_{\text{W}}$.

Acknowledgments

References

[1] Y. A. Gol'fand and E. P. Likhtman, "Extension of the Algebra of Poincaré Group Generators and Violation of p Invariance", *JETP Lett.* **13** (1971) 323.

[2] J. Wess and B. Zumino, "Supergauge transformations in four dimensions", *Nucl. Phys. B* **70** (1974) 39, `doi:10.1016/0550-3213(74)90355-1`.

[3] H. P. Nilles, "Supersymmetry, supergravity and particle physics", *Phys. Reports* **110** (1984) 1, `doi:10.1016/0370-1573(84)90008-5`.

[4] H. E. Haber and G. L. Kane, "The search for supersymmetry: Probing physics beyond the standard model", *Phys. Reports* **117** (1987) 75, `doi:10.1016/0370-1573(85)90051-1`.

[5] R. Barbieri, S. Ferrara, and C. A. Savoy, "Gauge models with spontaneously broken local supersymmetry", *Phys. Lett. B* **119** (1982) 343, `doi:10.1016/0370-2693(82)90685-2`.

[6] S. Dawson, E. Eichten, and C. Quigg, "Search for supersymmetric particles in hadron-hadron collisions", *Phys. Rev. D* **31** (1985) 1581, `doi:10.1103/PhysRevD.31.1581`.

[7] E. Witten, "Dynamical breaking of supersymmetry", *Nucl. Phys. B* **188** (1981) 513, `doi:10.1016/0550-3213(81)90006-7`.

[8] S. Dimopoulos and H. Georgi, "Softly broken supersymmetry and SU(5)", *Nucl. Phys. B* **193** (1981) 150, `doi:10.1016/0550-3213(81)90522-8`.

[9] ATLAS Collaboration, "Observation of a new particle in the search for the Standard Model Higgs boson with the ATLAS detector at the LHC", *Phys. Lett. B* **716** (2012) 1, `doi:10.1016/j.physletb.2012.08.020`, `arXiv:1207.7214`.

[10] CMS Collaboration, "Observation of a new boson with mass near 125 GeV in pp collisions at $\sqrt{s} = 7$ and 8 TeV", *JHEP* **06** (2013) 081, `doi:10.1007/JHEP06(2013)081`, `arXiv:1303.4571`.

[11] R. Barbieri and D. Pappadopulo, "S-particles at their naturalness limits", *JHEP* **10** (2009) 061, `doi:10.1088/1126-6708/2009/10/061`, `arXiv:0906.4546`.

[12] G. R. Farrar and P. Fayet, "Phenomenology of the production, decay, and detection of new hadronic states associated with supersymmetry", *Phys. Lett. B* **76** (1978) 575, `doi:10.1016/0370-2693(78)90858-4`.

[13] C. Boehm, A. Djouadi, and Y. Mambrini, "Decays of the lightest top squark", *Phys. Rev. D* **61** (2000) 095006, `doi:10.1103/PhysRevD.61.095006`, `arXiv:hep-ph/9907428`.

[14] C. Boehm, A. Djouadi, and M. Drees, "Light scalar top quarks and supersymmetric dark matter", *Phys. Rev. D* **62** (2000) 035012, `doi:10.1103/PhysRevD.62.035012`, `arXiv:hep-ph/9911496`.

[15] C. Balazs, M. S. Carena, and C. E. M. Wagner, "Dark matter, light stops and electroweak baryogenesis", *Phys. Rev. D* **70** (2004) 015007, `doi:10.1103/PhysRevD.70.015007`, `arXiv:hep-ph/0403224`.

[16] S. P. Martin, "Compressed supersymmetry and natural neutralino dark matter from top squark-mediated annihilation to top quarks", *Phys. Rev. D* **75** (2007) 115005, `doi:10.1103/PhysRevD.75.115005`, `arXiv:hep-ph/0703097`.

[17] S. P. Martin, "Top squark-mediated annihilation scenario and direct detection of dark matter in compressed supersymmetry", *Phys. Rev. D* **76** (2007) 095005, `doi:10.1103/PhysRevD.76.095005`, `arXiv:0707.2812`.

[18] M. Carena, A. Freitas, and C. E. M. Wagner, "Light stop searches at the LHC in events with one hard photon or jet and missing energy", *JHEP* **10** (2008) 109, `doi:10.1088/1126-6708/2008/10/109`, `arXiv:0808.2298`.

[19] R. Grober, M. M. Muhlleitner, E. Popenda, and A. Wlotzka, "Light stop decays: implications for LHC searches", *Eur. Phys. J. C* **75** (2015) 420, `doi:10.1140/epjc/s10052-015-3626-z`, `arXiv:1408.4662`.

[20] R. Grober, M. Muhlleitner, E. Popenda, and A. Wlotzka, "Light stop decays into $Wb\widetilde{\chi}_1^0$ near the kinematic threshold", *Phys. Lett. B* **747** (2015) 144, `doi:10.1016/j.physletb.2015.05.060`, `arXiv:1502.05935`.

[21] ATLAS Collaboration, "Search for new phenomena in final states with an energetic jet and large missing transverse momentum in pp collisions at $\sqrt{s} = 13$ TeV using the ATLAS detector", *Phys. Rev. D* **94** (2016) 032005, `doi:10.1103/PhysRevD.94.032005`, `arXiv:1604.07773`.

[22] ATLAS Collaboration, "Search for pair-produced third-generation squarks decaying via charm quarks or in compressed supersymmetric scenarios in pp collisions at $\sqrt{s} = 8$ TeV with the ATLAS detector", *Phys. Rev. D* **90** (2014) 052008, `doi:10.1103/PhysRevD.90.052008`, `arXiv:1407.0608`.

[23] CMS Collaboration, "Searches for third-generation squark production in fully hadronic final states in proton-proton collisions at $\sqrt{s} = 8$ TeV", *JHEP* **06** (2015) 116, `doi:10.1007/JHEP06(2015)116`, `arXiv:1503.08037`.

[24] CMS Collaboration, "CMS Luminosity Based on Pixel Cluster Counting - Summer 2012 Update", CMS Physics Analysis Summary CMS-PAS-LUM-12-001, 2012.

[25] CMS Collaboration, "Search for supersymmetry in pp collisions at 7 TeV in events with jets and missing transverse energy", *Phys. Lett. B* **698** (2011) 196, `doi:10.1016/j.physletb.2011.03.021`, `arXiv:1101.1628`.

[26] CMS Collaboration, "Search for Supersymmetry at the LHC in Events with Jets and Missing Transverse Energy", *Phys. Rev. Lett.* **107** (2011) 221804, `doi:10.1103/PhysRevLett.107.221804`, `arXiv:1109.2352`.

[27] CMS Collaboration, "Search for supersymmetry in final states with missing transverse energy and 0, 1, 2, or at least 3 b-quark jets in 7 TeV pp collisions using the variable α_T", *JHEP* **01** (2013) 077, `doi:10.1007/JHEP01(2013)077`, `arXiv:1210.8115`.

[28] CMS Collaboration, "Search for supersymmetry in hadronic final states with missing transverse energy using the variables α_T and b-quark multiplicity in pp collisions at $\sqrt{s} = 8$ TeV", *Eur. Phys. J. C* **73** (2013) 2568, `doi:10.1140/epjc/s10052-013-2568-6`, `arXiv:1303.2985`.

[29] ATLAS Collaboration, "Multi-channel search for squarks and gluinos in $\sqrt{s} = 7$ TeV pp collisions with the ATLAS detector", *Eur. Phys. J. C* **73** (2013) 2362, `doi:10.1140/epjc/s10052-013-2362-5`, `arXiv:1212.6149`.

[30] ATLAS Collaboration, "Search for a Supersymmetric Partner to the Top Quark in Final States with Jets and Missing Transverse Momentum at $\sqrt{s} = 7$ TeV with the ATLAS Detector", *Phys. Rev. Lett.* **109** (2012) 211802, `doi:10.1103/PhysRevLett.109.211802`, `arXiv:1208.1447`.

[31] ATLAS Collaboration, "Search for squarks and gluinos using final states with jets and missing transverse momentum with the ATLAS detector in $\sqrt{s} = 7$ TeV proton-proton collisions", *Phys. Lett. B* **710** (2012) 67, `doi:10.1016/j.physletb.2012.02.051`, `arXiv:1109.6572`.

[32] ATLAS Collaboration, "Search for top and bottom squarks from gluino pair production in final states with missing transverse energy and at least three b-jets with the ATLAS detector", *Eur. Phys. J. C* **72** (2012) 2174, `doi:10.1140/epjc/s10052-012-2174-z`, `arXiv:1207.4686`.

[33] ATLAS Collaboration, "Hunt for new phenomena using large jet multiplicities and missing transverse momentum with ATLAS in 4.7 fb^{-1} of $\sqrt{s} = 7$ TeV proton-proton collisions", *JHEP* **07** (2012) 167, `doi:10.1007/JHEP07(2012)167`, `arXiv:1206.1760`.

[34] ATLAS Collaboration, "Search for Scalar Bottom Quark Pair Production with the ATLAS Detector in pp Collisions at $\sqrt{s} = 7$ TeV", *Phys. Rev. Lett.* **108** (2012) 181802, `doi:10.1103/PhysRevLett.108.181802`, `arXiv:1112.3832`.

[35] ATLAS Collaboration, "Search for new phenomena in final states with large jet multiplicities and missing transverse momentum using $\sqrt{s} = 7$ TeV pp collisions with the ATLAS detector", *JHEP* **11** (2011) 099, `doi:10.1007/JHEP11(2011)099`, `arXiv:1110.2299`.

[36] ATLAS Collaboration, "Search for strong production of supersymmetric particles in final states with missing transverse momentum and at least three b-jets at $\sqrt{s} = 8$ TeV proton-proton collisions with the ATLAS detector", *JHEP* **10** (2014) 24, `doi:10.1007/JHEP10(2014)024`, `arXiv:1407.0600`.

[37] ATLAS Collaboration, "Search for squarks and gluinos with the ATLAS detector in final states with jets and missing transverse momentum using $\sqrt{s} = 8$ TeV proton–proton collision data", *JHEP* **09** (2014) 176, `doi:10.1007/JHEP09(2014)176`, `arXiv:1405.7875`.

[38] ATLAS Collaboration, "Search for direct third-generation squark pair production in final states with missing transverse momentum and two b-jets in $\sqrt{s} = 8$ TeV pp collisions with the ATLAS detector", *JHEP* **10** (2013) 189, `doi:10.1007/JHEP10(2013)189`, `arXiv:1308.2631`.

[39] ATLAS Collaboration, "Search for direct pair production of the top squark in all-hadronic final states in proton-proton collisions at $\sqrt{s} = 8$ TeV with the ATLAS detector", *JHEP* **09** (2014) 015, `doi:10.1007/JHEP09(2014)015`, `arXiv:1406.1122`.

[40] ATLAS Collaboration, "Search for new phenomena in final states with large jet multiplicities and missing transverse momentum with ATLAS using $\sqrt{s} = 13$ TeV proton–proton collisions", *Phys. Lett. B* **757** (2016) 334, `doi:10.1016/j.physletb.2016.04.005`, `arXiv:1602.06194`.

[41] ATLAS Collaboration, "Search for pair production of gluinos decaying via stop and sbottom in events with *b*-jets and large missing transverse momentum in *pp* collisions at $\sqrt{s} = 13$ TeV with the ATLAS detector", *Phys. Rev. D* **94** (2016) 032003, `doi:10.1103/PhysRevD.94.032003`, `arXiv:1605.09318`.

[42] ATLAS Collaboration, "Search for squarks and gluinos in final states with jets and missing transverse momentum at $\sqrt{s} = 13$ TeV with the ATLAS detector", *Eur. Phys. J. C* **76** (2016) 392, `doi:10.1140/epjc/s10052-016-4184-8`, `arXiv:1605.03814`.

[43] CMS Collaboration, "Search for supersymmetry in events with b-quark jets and missing transverse energy in pp collisions at 7 TeV", *Phys. Rev. D* **86** (2012) 072010, `doi:10.1103/PhysRevD.86.072010`, `arXiv:1208.4859`.

[44] CMS Collaboration, "Search for supersymmetry in hadronic final states using M_{T2} in pp collisions at $\sqrt{s} = 7$ TeV", *JHEP* **10** (2012) 018, `doi:10.1007/JHEP10(2012)018`, `arXiv:1207.1798`.

[45] CMS Collaboration, "Search for New Physics in the Multijet and Missing Transverse Momentum Final State in Proton-Proton Collisions at $\sqrt{s} = 7$ TeV", *Phys. Rev. Lett.* **109** (2012) 17180, `doi:10.1103/PhysRevLett.109.171803`, `arXiv:1207.1898`.

[46] CMS Collaboration, "Inclusive search for squarks and gluinos in pp collisions at $\sqrt{s} = 7$ TeV", *Phys. Rev. D* **85** (2012) 012004, `doi:10.1103/PhysRevD.85.012004`, `arXiv:1107.1279`.

[47] CMS Collaboration, "Search for supersymmetry with razor variables in pp collisions at $\sqrt{s} = 7$ TeV", *Phys. Rev. D* **90** (2014) 112001, `doi:10.1103/PhysRevD.90.112001`, `arXiv:1405.3961`.

[48] CMS Collaboration, "Inclusive search for supersymmetry using the razor variables in pp collisions at $\sqrt{s} = 7$ TeV", *Phys. Rev. Lett.* **111** (2013) 081802, `doi:10.1103/PhysRevLett.111.081802`, `arXiv:1212.6961`.

[49] CMS Collaboration, "Search for supersymmetry using razor variables in events with b-tagged jets in pp collisions at $\sqrt{s} = 8$ TeV", *Phys. Rev. D* **91** (2015) 052018, `doi:10.1103/PhysRevD.91.052018`, `arXiv:1502.00300`.

[50] CMS Collaboration, "Search for new physics in the multijet and missing transverse momentum final state in proton-proton collisions at $\sqrt{s} = 8$ TeV", *JHEP* **06** (2014) 055, `doi:10.1007/JHEP06(2014)055`, `arXiv:1402.4770`.

[51] CMS Collaboration, "Search for gluino mediated bottom- and top-squark production in multijet final states in pp collisions at 8 TeV", *Phys. Lett. B* **725** (2013) 243, `doi:10.1016/j.physletb.2013.06.058`, `arXiv:1305.2390`.

[52] CMS Collaboration, "Searches for supersymmetry using the M_{T2} variable in hadronic events produced in pp collisions at 8 TeV", *JHEP* **05** (2015) 078, `doi:10.1007/JHEP05(2015)078`, `arXiv:1502.04358`.

[53] CMS Collaboration, "Search for supersymmetry in the multijet and missing transverse momentum final state in pp collisions at 13 TeV", *Phys. Lett. B* **758** (2016) 152, `doi:10.1016/j.physletb.2016.05.002`, `arXiv:1602.06581`.

[54] CMS Collaboration, "Search for new physics with the M_{T2} variable in all-jets final states produced in pp collisions at $\sqrt{s} = 13$ TeV", *JHEP* **10** (2016) 006, `doi:10.1007/JHEP10(2016)006`, `arXiv:1603.04053`.

[55] ATLAS Collaboration, "ATLAS Run 1 searches for direct pair production of third-generation squarks at the Large Hadron Collider", *Eur. Phys. J. C* **75** (2015) 510, `doi:10.1140/epjc/s10052-015-3726-9`, `arXiv:1506.08616`. [Erratum: `doi:10.1140/epjc/s10052-016-3935-x`].

[56] CMS Collaboration, "Search for direct pair production of scalar top quarks in the single-and dilepton channels in proton-proton collisions at $\sqrt{s} = 8$ TeV", *JHEP* **07** (2016) 027, `doi:10.1007/JHEP07(2016)027`, `arXiv:1602.03169`.

[57] ATLAS Collaboration, "Search for top squarks in final states with one isolated lepton, jets, and missing transverse momentum in $\sqrt{s} = 13$ TeV pp collisions with the ATLAS detector", *Phys. Rev. D* **94** (2016) 052009, `doi:10.1103/PhysRevD.94.052009`, `arXiv:1606.03903`.

[58] J. Alwall, P. Schuster, and N. Toro, "Simplified models for a first characterization of new physics at the LHC", *Phys. Rev. D* **79** (2009) 075020, `doi:10.1103/PhysRevD.79.075020`, `arXiv:0810.3921`.

[59] J. Alwall, M.-P. Le, M. Lisanti, and J. G. Wacker, "Model-independent jets plus missing energy searches", *Phys. Rev. D* **79** (2009) 015005, `doi:10.1103/PhysRevD.79.015005`, `arXiv:0809.3264`.

[60] LHC New Physics Working Group Collaboration, "Simplified models for LHC new physics searches", *J. Phys. G* **39** (2012) 105005, `doi:10.1088/0954-3899/39/10/105005`, `arXiv:1105.2838`.

[61] CMS Collaboration, "Data Parking and Data Scouting at the CMS Experiment", CMS Detector Performance Note CMS-DP-2012-022, CERN-CMS-DP-2012-022, 2012.

[62] CMS Collaboration, "Description and performance of track and primary-vertex reconstruction with the CMS tracker", *JINST* **9** (2014) P10009, `doi:10.1088/1748-0221/9/10/P10009`, `arXiv:1405.6569`.

[63] CMS Collaboration, "Performance of CMS muon reconstruction in pp collision events at $\sqrt{s} = 7$ TeV", *J. Instrum.* **7** (2012) P10002, `doi:10.1088/1748-0221/7/10/P10002`.

[64] CMS Collaboration, "The CMS experiment at the CERN LHC", *JINST* **3** (2008) S08004, `doi:10.1088/1748-0221/3/08/S08004`.

[65] L. Randall and D. Tucker-Smith, "Dijet Searches for Supersymmetry at the Large Hadron Collider", *Phys. Rev. Lett.* **101** (2008) 221803, `doi:10.1103/PhysRevLett.101.221803`, `arXiv:0806.1049`.

[66] CMS Collaboration, "Performance of electron reconstruction and selection with the CMS detector in proton-proton collisions at $\sqrt{s} = 8$ TeV", *JINST* **10** (2015) P06005, `doi:10.1088/1748-0221/10/06/P06005`, `arXiv:1502.02701`.

[67] CMS Collaboration, "Search for top-squark pair production in the single-lepton final state in pp collisions at $\sqrt{s} = 8$ TeV", *Eur. Phys. J. C* **73** (2013) 2677, `doi:10.1140/epjc/s10052-013-2677-2`, `arXiv:1308.1586`.

[68] CMS Collaboration, "Performance of photon reconstruction and identification with the CMS detector in proton-proton collisions at $\sqrt{s} = 8$ TeV", *JINST* **10** (2015) P08010, `doi:10.1088/1748-0221/10/08/P08010`, `arXiv:1502.02702`.

[69] M. Cacciari, G. P. Salam, and G. Soyez, "The anti-k_t jet clustering algorithm", *JHEP* **04** (2008) 063, `doi:10.1088/1126-6708/2008/04/063`, `arXiv:0802.1189`.

[70] CMS Collaboration, "Determination of jet energy calibration and transverse momentum resolution in CMS", *JINST* **6** (2011) P11002, `doi:10.1088/1748-0221/6/11/P11002`, `arXiv:1107.4277`.

[71] CMS Collaboration, "Identification of b-quark jets with the CMS experiment", *JINST* **8** (2013) P04013, `doi:10.1088/1748-0221/8/04/P04013`, `arXiv:1211.4462`.

[72] CMS Collaboration, "identification and filtering of uncharacteristic noise in the CMS hadron calorimeter", *JINST* **5** (2010) T03014, `doi:10.1088/1748-0221/5/03/T03014`, `arXiv:0911.4881`.

[73] CMS Collaboration, "Missing transverse energy performance of the CMS detector", *JINST* **6** (2011) P09001, `doi:10.1088/1748-0221/6/09/P09001`, `arXiv:1106.5048`.

[74] CMS Collaboration, "Particle–Flow Event Reconstruction in CMS and Performance for Jets, Taus, and E_T^{miss}", CMS Physics Analysis Summary CMS-PAS-PFT-09-001, 2009.

[75] CMS Collaboration, "Commissioning of the particle-flow event reconstruction with the first LHC collisions recorded in the CMS detector", CMS Physics Analysis Summary CMS-PAS-PFT-10-001, 2010.

[76] J. Alwall et al., "MadGraph 5: going beyond", *JHEP* **06** (2011) 128, `doi:10.1007/JHEP06(2011)128`, `arXiv:1106.0522`.

[77] S. Frixione, P. Nason, and C. Oleari, "Matching NLO QCD computations with parton shower simulations: the POWHEG method", *JHEP* **11** (2007) 070, `doi:10.1088/1126-6708/2007/11/070`, `arXiv:0709.2092`.

[78] P. Nason, "A New method for combining NLO QCD with shower Monte Carlo algorithms", *JHEP* **11** (2004) 040, `doi:10.1088/1126-6708/2004/11/040`, `arXiv:hep-ph/0409146`.

[79] S. Alioli, P. Nason, C. Oleari, and E. Re, "A general framework for implementing NLO calculations in shower Monte Carlo programs: the POWHEG BOX", *JHEP* **06** (2010) 043, `doi:10.1007/JHEP06(2010)043`, `arXiv:1002.2581`.

[80] S. Frixione, P. Nason, and G. Ridolfi, "A positive-weight next-to-leading-order Monte Carlo for heavy flavour hadroproduction", *JHEP* **09** (2007) 126, `doi:10.1088/1126-6708/2007/09/126`, `arXiv:0707.3088`.

[81] T. Sjöstrand, S. Mrenna, and P. Z. Skands, "PYTHIA 6.4 physics and manual", *JHEP* **05** (2006) 026, `doi:10.1088/1126-6708/2006/05/026`, `arXiv:hep-ph/0603175`.

[82] J. Pumplin et al., "New generation of parton distributions with uncertainties from global QCD analysis", *JHEP* **07** (2002) 012, `doi:10.1088/1126-6708/2002/07/012`, `arXiv:hep-ph/0201195`.

[83] H.-L. Lai et al., "New parton distributions for collider physics", *Phys. Rev. D* **82** (2010) 074024, `doi:10.1103/PhysRevD.82.074024`, `arXiv:1007.2241`.

[84] GEANT4 Collaboration, "GEANT4—a simulation toolkit", *Nucl. Instrum. Meth. A* **506** (2003) 250, `doi:10.1016/S0168-9002(03)01368-8`.

[85] R. Gavin, Y. Li, F. Petriello, and S. Quackenbush, "FEWZ 2.0: A code for hadronic Z production at next-to-next-to-leading order", *Comput. Phys. Commun.* **182** (2011) 2388, `doi:10.1016/j.cpc.2011.06.008`, `arXiv:1011.3540`.

[86] R. Gavin, Y. Li, F. Petriello, and S. Quackenbush, "W Physics at the LHC with FEWZ 2.1", *Comput. Phys. Commun.* **184** (2013) 208, `doi:10.1016/j.cpc.2012.09.005`, `arXiv:1201.5896`.

[87] J. M. Campbell, R. K. Ellis, and C. Williams, "Vector boson pair production at the LHC", *JHEP* **07** (2011) 018, `doi:10.1007/JHEP07(2011)018`, `arXiv:1105.0020`.

[88] N. Kidonakis, "Next-to-next-to-leading-order collinear and soft gluon corrections for t-channel single top quark production", *Phys. Rev. D* **83** (2011) 091503, `doi:10.1103/PhysRevD.83.091503`, `arXiv:1103.2792`.

[89] M. Czakon and A. Mitov, "Top++: A Program for the Calculation of the Top-Pair Cross-Section at Hadron Colliders", *Comput. Phys. Commun.* **185** (2014) 2930, `doi:10.1016/j.cpc.2014.06.021`, `arXiv:1112.5675`.

[90] Z. Bern et al., "Driving missing data at next-to-leading order", *Phys. Rev. D* **84** (2011) 114002, `doi:10.1103/PhysRevD.84.114002`, `arXiv:1106.1423`.

[91] J. K. Lindsey, "Parametric Statistical Inference". Oxford University Press, 1996. ISBN 0-19-852359-9.

[92] A. L. Read, "Presentation of search results: the CL_s technique", *J. Phys. G* **28** (2002) 2693, `doi:10.1088/0954-3899/28/10/313`.

[93] T. Junk, "Confidence level computation for combining searches with small statistics", *Nucl. Instrum. Meth. A* **434** (1999) 435, `doi:10.1016/S0168-9002(99)00498-2`, `arXiv:hep-ex/9902006`.

[94] ATLAS and CMS Collaborations, LHC Higgs Combination Group, "Procedure for the LHC Higgs boson search combination in Summer 2011", (2011). Technical Report ATL-PHYS-PUB 2011-11, CMS NOTE 2011/005.

[95] W. Beenakker, R. Höpker, M. Spira, and P. M. Zerwas, "Squark and gluino production at hadron colliders", *Nucl. Phys. B* **492** (1997) 51, `doi:10.1016/S0550-3213(97)80027-2`, `arXiv:hep-ph/9610490`.

[96] A. Kulesza and L. Motyka, "Soft gluon resummation for the production of gluino-gluino and squark-antisquark pairs at the LHC", *Phys. Rev. D* **80** (2009) 095004, `doi:10.1103/PhysRevD.80.095004`, `arXiv:0905.4749`.

[97] A. Kulesza and L. Motyka, "Threshold Resummation for Squark-Antisquark and Gluino-Pair Production at the LHC", *Phys. Rev. Lett.* **102** (2009) 111802, `doi:10.1103/PhysRevLett.102.111802`, `arXiv:0807.2405`.

[98] W. Beenakker et al., "Soft-gluon resummation for squark and gluino hadroproduction", *JHEP* **12** (2009) 041, `doi:10.1088/1126-6708/2009/12/041`, `arXiv:0909.4418`.

[99] W. Beenakker et al., "Squark and gluino hadroproduction", *Int. J. Mod. Phys. A* **26** (2011) 2637, `doi:10.1142/S0217751X11053560`, `arXiv:1105.1110`.

[100] M. Krämer et al., "Supersymmetry production cross sections in pp collisions at $\sqrt{s} = 7\,\mathrm{TeV}$", (2012). `arXiv:1206.2892`.

[101] CMS Collaboration, "The fast simulation of the CMS detector at LHC", *J. Phys. Conf. Ser.* **331** (2011) 032049, `doi:10.1088/1742-6596/331/3/032049`.

[102] LEP2 SUSY working group (ALEPH, DELPHI, L3 and OPAL experiments), "Combined LEP Chargino Results, up to 208 GeV for large m_0", (2001). Note LEPSUSYWG/01-03.1.

[103] LEP2 SUSY working group (ALEPH, DELPHI, L3 and OPAL experiments), "Combined LEP Chargino Results, up to 208 GeV for low DM", (2004). Note LEPSUSYWG/02-04.1.

[104] M. Perelstein and A. Weiler, "Polarized Tops from Stop Decays at the LHC", *JHEP* **03** (2009) 141, `doi:10.1088/1126-6708/2009/03/141`, `arXiv:0811.1024`.

A The CMS Collaboration

Yerevan Physics Institute, Yerevan, Armenia
V. Khachatryan, A.M. Sirunyan, A. Tumasyan

Institut für Hochenergiephysik der OeAW, Wien, Austria
W. Adam, E. Asilar, T. Bergauer, J. Brandstetter, E. Brondolin, M. Dragicevic, J. Erö, M. Flechl, M. Friedl, R. Frühwirth[1], V.M. Ghete, C. Hartl, N. Hörmann, J. Hrubec, M. Jeitler[1], A. König, M. Krammer[1], I. Krätschmer, D. Liko, T. Matsushita, I. Mikulec, D. Rabady, N. Rad, B. Rahbaran, H. Rohringer, J. Schieck[1], J. Strauss, W. Treberer-Treberspurg, W. Waltenberger, C.-E. Wulz[1]

National Centre for Particle and High Energy Physics, Minsk, Belarus
V. Mossolov, N. Shumeiko, J. Suarez Gonzalez

Universiteit Antwerpen, Antwerpen, Belgium
S. Alderweireldt, T. Cornelis, E.A. De Wolf, X. Janssen, A. Knutsson, J. Lauwers, S. Luyckx, M. Van De Klundert, H. Van Haevermaet, P. Van Mechelen, N. Van Remortel, A. Van Spilbeeck

Vrije Universiteit Brussel, Brussel, Belgium
S. Abu Zeid, F. Blekman, J. D'Hondt, N. Daci, I. De Bruyn, K. Deroover, N. Heracleous, J. Keaveney, S. Lowette, S. Moortgat, L. Moreels, A. Olbrechts, Q. Python, D. Strom, S. Tavernier, W. Van Doninck, P. Van Mulders, I. Van Parijs

Université Libre de Bruxelles, Bruxelles, Belgium
H. Brun, C. Caillol, B. Clerbaux, G. De Lentdecker, G. Fasanella, L. Favart, R. Goldouzian, A. Grebenyuk, G. Karapostoli, T. Lenzi, A. Léonard, T. Maerschalk, A. Marinov, A. Randle-conde, T. Seva, C. Vander Velde, P. Vanlaer, R. Yonamine, F. Zenoni, F. Zhang[2]

Ghent University, Ghent, Belgium
L. Benucci, A. Cimmino, S. Crucy, D. Dobur, A. Fagot, G. Garcia, M. Gul, J. Mccartin, A.A. Ocampo Rios, D. Poyraz, D. Ryckbosch, S. Salva, R. Schöfbeck, M. Sigamani, M. Tytgat, W. Van Driessche, E. Yazgan, N. Zaganidis

Université Catholique de Louvain, Louvain-la-Neuve, Belgium
C. Beluffi[3], O. Bondu, S. Brochet, G. Bruno, A. Caudron, L. Ceard, S. De Visscher, C. Delaere, M. Delcourt, L. Forthomme, B. Francois, A. Giammanco, A. Jafari, P. Jez, M. Komm, V. Lemaitre, A. Magitteri, A. Mertens, M. Musich, C. Nuttens, K. Piotrzkowski, L. Quertenmont, M. Selvaggi, M. Vidal Marono, S. Wertz

Université de Mons, Mons, Belgium
N. Beliy, G.H. Hammad

Centro Brasileiro de Pesquisas Fisicas, Rio de Janeiro, Brazil
W.L. Aldá Júnior, F.L. Alves, G.A. Alves, L. Brito, M. Correa Martins Junior, M. Hamer, C. Hensel, A. Moraes, M.E. Pol, P. Rebello Teles

Universidade do Estado do Rio de Janeiro, Rio de Janeiro, Brazil
E. Belchior Batista Das Chagas, W. Carvalho, J. Chinellato[4], A. Custódio, E.M. Da Costa, D. De Jesus Damiao, C. De Oliveira Martins, S. Fonseca De Souza, L.M. Huertas Guativa, H. Malbouisson, D. Matos Figueiredo, C. Mora Herrera, L. Mundim, H. Nogima, W.L. Prado Da Silva, A. Santoro, A. Sznajder, E.J. Tonelli Manganote[4], A. Vilela Pereira

Universidade Estadual Paulista [a], Universidade Federal do ABC [b], São Paulo, Brazil
S. Ahuja[a], C.A. Bernardes[b], A. De Souza Santos[b], S. Dogra[a], T.R. Fernandez Perez Tomei[a],

E.M. Gregores[b], P.G. Mercadante[b], C.S. Moon[a,5], S.F. Novaes[a], Sandra S. Padula[a], D. Romero Abad[b], J.C. Ruiz Vargas

Institute for Nuclear Research and Nuclear Energy, Sofia, Bulgaria
A. Aleksandrov, R. Hadjiiska, P. Iaydjiev, M. Rodozov, S. Stoykova, G. Sultanov, M. Vutova

University of Sofia, Sofia, Bulgaria
A. Dimitrov, I. Glushkov, L. Litov, B. Pavlov, P. Petkov

Beihang University, Beijing, China
W. Fang[6]

Institute of High Energy Physics, Beijing, China
M. Ahmad, J.G. Bian, G.M. Chen, H.S. Chen, M. Chen, T. Cheng, R. Du, C.H. Jiang, D. Leggat, R. Plestina[7], F. Romeo, S.M. Shaheen, A. Spiezia, J. Tao, C. Wang, Z. Wang, H. Zhang

State Key Laboratory of Nuclear Physics and Technology, Peking University, Beijing, China
C. Asawatangtrakuldee, Y. Ban, Q. Li, S. Liu, Y. Mao, S.J. Qian, D. Wang, Z. Xu

Universidad de Los Andes, Bogota, Colombia
C. Avila, A. Cabrera, L.F. Chaparro Sierra, C. Florez, J.P. Gomez, B. Gomez Moreno, J.C. Sanabria

University of Split, Faculty of Electrical Engineering, Mechanical Engineering and Naval Architecture, Split, Croatia
N. Godinovic, D. Lelas, I. Puljak, P.M. Ribeiro Cipriano

University of Split, Faculty of Science, Split, Croatia
Z. Antunovic, M. Kovac

Institute Rudjer Boskovic, Zagreb, Croatia
V. Brigljevic, D. Ferencek, K. Kadija, J. Luetic, S. Micanovic, L. Sudic

University of Cyprus, Nicosia, Cyprus
A. Attikis, G. Mavromanolakis, J. Mousa, C. Nicolaou, F. Ptochos, P.A. Razis, H. Rykaczewski

Charles University, Prague, Czech Republic
M. Finger[8], M. Finger Jr.[8]

Universidad San Francisco de Quito, Quito, Ecuador
E. Carrera Jarrin

Academy of Scientific Research and Technology of the Arab Republic of Egypt, Egyptian Network of High Energy Physics, Cairo, Egypt
Y. Assran[9,10], A. Ellithi Kamel[11,11], A. Mahrous[12], A. Radi[10,13]

National Institute of Chemical Physics and Biophysics, Tallinn, Estonia
B. Calpas, M. Kadastik, M. Murumaa, L. Perrini, M. Raidal, A. Tiko, C. Veelken

Department of Physics, University of Helsinki, Helsinki, Finland
P. Eerola, J. Pekkanen, M. Voutilainen

Helsinki Institute of Physics, Helsinki, Finland
J. Härkönen, V. Karimäki, R. Kinnunen, T. Lampén, K. Lassila-Perini, S. Lehti, T. Lindén, P. Luukka, T. Peltola, J. Tuominiemi, E. Tuovinen, L. Wendland

Lappeenranta University of Technology, Lappeenranta, Finland
J. Talvitie, T. Tuuva

DSM/IRFU, CEA/Saclay, Gif-sur-Yvette, France
M. Besancon, F. Couderc, M. Dejardin, D. Denegri, B. Fabbro, J.L. Faure, C. Favaro, F. Ferri, S. Ganjour, A. Givernaud, P. Gras, G. Hamel de Monchenault, P. Jarry, E. Locci, M. Machet, J. Malcles, J. Rander, A. Rosowsky, M. Titov, A. Zghiche

Laboratoire Leprince-Ringuet, Ecole Polytechnique, IN2P3-CNRS, Palaiseau, France
A. Abdulsalam, I. Antropov, S. Baffioni, F. Beaudette, P. Busson, L. Cadamuro, E. Chapon, C. Charlot, O. Davignon, L. Dobrzynski, R. Granier de Cassagnac, M. Jo, S. Lisniak, P. Miné, I.N. Naranjo, M. Nguyen, C. Ochando, G. Ortona, P. Paganini, P. Pigard, S. Regnard, R. Salerno, Y. Sirois, T. Strebler, Y. Yilmaz, A. Zabi

Institut Pluridisciplinaire Hubert Curien, Université de Strasbourg, Université de Haute Alsace Mulhouse, CNRS/IN2P3, Strasbourg, France
J.-L. Agram[14], J. Andrea, A. Aubin, D. Bloch, J.-M. Brom, M. Buttignol, E.C. Chabert, N. Chanon, C. Collard, E. Conte[14], X. Coubez, J.-C. Fontaine[14], D. Gelé, U. Goerlach, C. Goetzmann, A.-C. Le Bihan, J.A. Merlin[15], K. Skovpen, P. Van Hove

Centre de Calcul de l'Institut National de Physique Nucleaire et de Physique des Particules, CNRS/IN2P3, Villeurbanne, France
S. Gadrat

Université de Lyon, Université Claude Bernard Lyon 1, CNRS-IN2P3, Institut de Physique Nucléaire de Lyon, Villeurbanne, France
S. Beauceron, C. Bernet, G. Boudoul, E. Bouvier, C.A. Carrillo Montoya, R. Chierici, D. Contardo, B. Courbon, P. Depasse, H. El Mamouni, J. Fan, J. Fay, S. Gascon, M. Gouzevitch, B. Ille, F. Lagarde, I.B. Laktineh, M. Lethuillier, L. Mirabito, A.L. Pequegnot, S. Perries, A. Popov[16], J.D. Ruiz Alvarez, D. Sabes, V. Sordini, M. Vander Donckt, P. Verdier, S. Viret

Georgian Technical University, Tbilisi, Georgia
T. Toriashvili[17]

Tbilisi State University, Tbilisi, Georgia
Z. Tsamalaidze[8]

RWTH Aachen University, I. Physikalisches Institut, Aachen, Germany
C. Autermann, S. Beranek, L. Feld, A. Heister, M.K. Kiesel, K. Klein, M. Lipinski, A. Ostapchuk, M. Preuten, F. Raupach, S. Schael, C. Schomakers, J.F. Schulte, J. Schulz, T. Verlage, H. Weber, V. Zhukov[16]

RWTH Aachen University, III. Physikalisches Institut A, Aachen, Germany
M. Ata, M. Brodski, E. Dietz-Laursonn, D. Duchardt, M. Endres, M. Erdmann, S. Erdweg, T. Esch, R. Fischer, A. Güth, T. Hebbeker, C. Heidemann, K. Hoepfner, S. Knutzen, M. Merschmeyer, A. Meyer, P. Millet, S. Mukherjee, M. Olschewski, K. Padeken, P. Papacz, T. Pook, M. Radziej, H. Reithler, M. Rieger, F. Scheuch, L. Sonnenschein, D. Teyssier, S. Thüer

RWTH Aachen University, III. Physikalisches Institut B, Aachen, Germany
V. Cherepanov, Y. Erdogan, G. Flügge, H. Geenen, M. Geisler, F. Hoehle, B. Kargoll, T. Kress, A. Künsken, J. Lingemann, A. Nehrkorn, A. Nowack, I.M. Nugent, C. Pistone, O. Pooth, A. Stahl[15]

Deutsches Elektronen-Synchrotron, Hamburg, Germany
M. Aldaya Martin, I. Asin, K. Beernaert, O. Behnke, U. Behrens, K. Borras[18], A. Campbell, P. Connor, C. Contreras-Campana, F. Costanza, C. Diez Pardos, G. Dolinska, S. Dooling, G. Eckerlin, D. Eckstein, T. Eichhorn, E. Gallo[19], J. Garay Garcia, A. Geiser, A. Gizhko,

J.M. Grados Luyando, P. Gunnellini, A. Harb, J. Hauk, M. Hempel[20], H. Jung, A. Kalogeropoulos, O. Karacheban[20], M. Kasemann, J. Kieseler, C. Kleinwort, I. Korol, W. Lange, A. Lelek, J. Leonard, K. Lipka, A. Lobanov, W. Lohmann[20], R. Mankel, I.-A. Melzer-Pellmann, A.B. Meyer, G. Mittag, J. Mnich, A. Mussgiller, E. Ntomari, D. Pitzl, R. Placakyte, A. Raspereza, B. Roland, M.Ö. Sahin, P. Saxena, T. Schoerner-Sadenius, C. Seitz, S. Spannagel, N. Stefaniuk, K.D. Trippkewitz, G.P. Van Onsem, R. Walsh, C. Wissing

University of Hamburg, Hamburg, Germany
V. Blobel, M. Centis Vignali, A.R. Draeger, T. Dreyer, J. Erfle, E. Garutti, K. Goebel, D. Gonzalez, M. Görner, J. Haller, M. Hoffmann, R.S. Höing, A. Junkes, R. Klanner, R. Kogler, N. Kovalchuk, T. Lapsien, T. Lenz, I. Marchesini, D. Marconi, M. Meyer, M. Niedziela, D. Nowatschin, J. Ott, F. Pantaleo[15], T. Peiffer, A. Perieanu, N. Pietsch, J. Poehlsen, C. Sander, C. Scharf, P. Schleper, E. Schlieckau, A. Schmidt, S. Schumann, J. Schwandt, H. Stadie, G. Steinbrück, F.M. Stober, H. Tholen, D. Troendle, E. Usai, L. Vanelderen, A. Vanhoefer, B. Vormwald

Institut für Experimentelle Kernphysik, Karlsruhe, Germany
C. Barth, C. Baus, J. Berger, C. Böser, E. Butz, T. Chwalek, F. Colombo, W. De Boer, A. Descroix, A. Dierlamm, S. Fink, F. Frensch, R. Friese, M. Giffels, A. Gilbert, D. Haitz, F. Hartmann[15], S.M. Heindl, U. Husemann, I. Katkov[16], A. Kornmayer[15], P. Lobelle Pardo, B. Maier, H. Mildner, M.U. Mozer, T. Müller, Th. Müller, M. Plagge, G. Quast, K. Rabbertz, S. Röcker, F. Roscher, M. Schröder, G. Sieber, H.J. Simonis, R. Ulrich, J. Wagner-Kuhr, S. Wayand, M. Weber, T. Weiler, S. Williamson, C. Wöhrmann, R. Wolf

Institute of Nuclear and Particle Physics (INPP), NCSR Demokritos, Aghia Paraskevi, Greece
G. Anagnostou, G. Daskalakis, T. Geralis, V.A. Giakoumopoulou, A. Kyriakis, D. Loukas, A. Psallidas, I. Topsis-Giotis

National and Kapodistrian University of Athens, Athens, Greece
A. Agapitos, S. Kesisoglou, A. Panagiotou, N. Saoulidou, E. Tziaferi

University of Ioánnina, Ioánnina, Greece
I. Evangelou, G. Flouris, C. Foudas, P. Kokkas, N. Loukas, N. Manthos, I. Papadopoulos, E. Paradas, J. Strologas

MTA-ELTE Lendület CMS Particle and Nuclear Physics Group, Eötvös Loránd University
N. Filipovic

Wigner Research Centre for Physics, Budapest, Hungary
G. Bencze, C. Hajdu, P. Hidas, D. Horvath[21], F. Sikler, V. Veszpremi, G. Vesztergombi[22], A.J. Zsigmond

Institute of Nuclear Research ATOMKI, Debrecen, Hungary
N. Beni, S. Czellar, J. Karancsi[23], J. Molnar, Z. Szillasi

University of Debrecen, Debrecen, Hungary
M. Bartók[22], A. Makovec, P. Raics, Z.L. Trocsanyi, B. Ujvari

National Institute of Science Education and Research, Bhubaneswar, India
S. Choudhury[24], P. Mal, K. Mandal, A. Nayak, D.K. Sahoo, N. Sahoo, S.K. Swain

Panjab University, Chandigarh, India
S. Bansal, S.B. Beri, V. Bhatnagar, R. Chawla, R. Gupta, U.Bhawandeep, A.K. Kalsi, A. Kaur, M. Kaur, R. Kumar, A. Mehta, M. Mittal, J.B. Singh, G. Walia

University of Delhi, Delhi, India
Ashok Kumar, A. Bhardwaj, B.C. Choudhary, R.B. Garg, S. Keshri, A. Kumar, S. Malhotra, M. Naimuddin, N. Nishu, K. Ranjan, R. Sharma, V. Sharma

Saha Institute of Nuclear Physics, Kolkata, India
R. Bhattacharya, S. Bhattacharya, K. Chatterjee, S. Dey, S. Dutta, S. Ghosh, N. Majumdar, A. Modak, K. Mondal, S. Mukhopadhyay, S. Nandan, A. Purohit, A. Roy, D. Roy, S. Roy Chowdhury, S. Sarkar, M. Sharan

Bhabha Atomic Research Centre, Mumbai, India
R. Chudasama, D. Dutta, V. Jha, V. Kumar, A.K. Mohanty[15], L.M. Pant, P. Shukla, A. Topkar

Tata Institute of Fundamental Research, Mumbai, India
T. Aziz, S. Banerjee, S. Bhowmik[25], R.M. Chatterjee, R.K. Dewanjee, S. Dugad, S. Ganguly, S. Ghosh, M. Guchait, A. Gurtu[26], Sa. Jain, G. Kole, S. Kumar, B. Mahakud, M. Maity[25], G. Majumder, K. Mazumdar, S. Mitra, G.B. Mohanty, B. Parida, T. Sarkar[25], N. Sur, B. Sutar, N. Wickramage[27]

Indian Institute of Science Education and Research (IISER), Pune, India
S. Chauhan, S. Dube, A. Kapoor, K. Kothekar, A. Rane, S. Sharma

Institute for Research in Fundamental Sciences (IPM), Tehran, Iran
H. Bakhshiansohi, H. Behnamian, S.M. Etesami[28], A. Fahim[29], M. Khakzad, M. Mohammadi Najafabadi, M. Naseri, S. Paktinat Mehdiabadi, F. Rezaei Hosseinabadi, B. Safarzadeh[30], M. Zeinali

University College Dublin, Dublin, Ireland
M. Felcini, M. Grunewald

INFN Sezione di Bari ^{a}, Università di Bari ^{b}, Politecnico di Bari ^{c}, Bari, Italy
M. Abbrescia^{a,b}, C. Calabria^{a,b}, C. Caputo^{a,b}, A. Colaleo^a, D. Creanza^{a,c}, L. Cristella^{a,b}, N. De Filippis^{a,c}, M. De Palma^{a,b}, L. Fiore^a, G. Iaselli^{a,c}, G. Maggi^{a,c}, M. Maggi^a, G. Miniello^{a,b}, S. My^{a,b}, S. Nuzzo^{a,b}, A. Pompili^{a,b}, G. Pugliese^{a,c}, R. Radogna^{a,b}, A. Ranieri^a, G. Selvaggi^{a,b}, L. Silvestris^{a,15}, R. Venditti^{a,b}

INFN Sezione di Bologna ^{a}, Università di Bologna ^{b}, Bologna, Italy
G. Abbiendi^a, C. Battilana, D. Bonacorsi^{a,b}, S. Braibant-Giacomelli^{a,b}, L. Brigliadori^{a,b}, R. Campanini^{a,b}, P. Capiluppi^{a,b}, A. Castro^{a,b}, F.R. Cavallo^a, S.S. Chhibra^{a,b}, G. Codispoti^{a,b}, M. Cuffiani^{a,b}, G.M. Dallavalle^a, F. Fabbri^a, A. Fanfani^{a,b}, D. Fasanella^{a,b}, P. Giacomelli^a, C. Grandi^a, L. Guiducci^{a,b}, S. Marcellini^a, G. Masetti^a, A. Montanari^a, F.L. Navarria^{a,b}, A. Perrotta^a, A.M. Rossi^{a,b}, T. Rovelli^{a,b}, G.P. Siroli^{a,b}, N. Tosi^{a,b,15}

INFN Sezione di Catania ^{a}, Università di Catania ^{b}, Catania, Italy
G. Cappello^b, M. Chiorboli^{a,b}, S. Costa^{a,b}, A. Di Mattia^a, F. Giordano^{a,b}, R. Potenza^{a,b}, A. Tricomi^{a,b}, C. Tuve^{a,b}

INFN Sezione di Firenze ^{a}, Università di Firenze ^{b}, Firenze, Italy
G. Barbagli^a, V. Ciulli^{a,b}, C. Civinini^a, R. D'Alessandro^{a,b}, E. Focardi^{a,b}, V. Gori^{a,b}, P. Lenzi^{a,b}, M. Meschini^a, S. Paoletti^a, G. Sguazzoni^a, L. Viliani^{a,b,15}

INFN Laboratori Nazionali di Frascati, Frascati, Italy
L. Benussi, S. Bianco, F. Fabbri, D. Piccolo, F. Primavera[15]

INFN Sezione di Genova ^{a}, Università di Genova ^{b}, Genova, Italy
V. Calvelli^{a,b}, F. Ferro^a, M. Lo Vetere^{a,b}, M.R. Monge^{a,b}, E. Robutti^a, S. Tosi^{a,b}

INFN Sezione di Milano-Bicocca [a]**, Università di Milano-Bicocca** [b]**, Milano, Italy**
L. Brianza, M.E. Dinardo[a,b], S. Fiorendi[a,b], S. Gennai[a], A. Ghezzi[a,b], P. Govoni[a,b], S. Malvezzi[a], R.A. Manzoni[a,b,15], B. Marzocchi[a,b], D. Menasce[a], L. Moroni[a], M. Paganoni[a,b], D. Pedrini[a], S. Pigazzini, S. Ragazzi[a,b], N. Redaelli[a], T. Tabarelli de Fatis[a,b]

INFN Sezione di Napoli [a]**, Università di Napoli 'Federico II'** [b]**, Napoli, Italy, Università della Basilicata** [c]**, Potenza, Italy, Università G. Marconi** [d]**, Roma, Italy**
S. Buontempo[a], N. Cavallo[a,c], S. Di Guida[a,d,15], M. Esposito[a,b], F. Fabozzi[a,c], A.O.M. Iorio[a,b], G. Lanza[a], L. Lista[a], S. Meola[a,d,15], M. Merola[a], P. Paolucci[a,15], C. Sciacca[a,b], F. Thyssen

INFN Sezione di Padova [a]**, Università di Padova** [b]**, Padova, Italy, Università di Trento** [c]**, Trento, Italy**
P. Azzi[a,15], N. Bacchetta[a], L. Benato[a,b], A. Boletti[a,b], A. Branca[a,b], M. Dall'Osso[a,b], P. De Castro Manzano[a], T. Dorigo[a], F. Fanzago[a], F. Gonella[a], A. Gozzelino[a], M. Gulmini[a,31], K. Kanishchev[a,c], S. Lacaprara[a], M. Margoni[a,b], A.T. Meneguzzo[a,b], F. Montecassiano[a], M. Passaseo[a], J. Pazzini[a,b,15], M. Pegoraro[a], N. Pozzobon[a,b], P. Ronchese[a,b], F. Simonetto[a,b], E. Torassa[a], M. Tosi[a,b], S. Ventura[a], M. Zanetti, P. Zotto[a,b], A. Zucchetta[a,b], G. Zumerle[a,b]

INFN Sezione di Pavia [a]**, Università di Pavia** [b]**, Pavia, Italy**
A. Braghieri[a], A. Magnani[a,b], P. Montagna[a,b], S.P. Ratti[a,b], V. Re[a], C. Riccardi[a,b], P. Salvini[a], I. Vai[a,b], P. Vitulo[a,b]

INFN Sezione di Perugia [a]**, Università di Perugia** [b]**, Perugia, Italy**
L. Alunni Solestizi[a,b], G.M. Bilei[a], D. Ciangottini[a,b], L. Fanò[a,b], P. Lariccia[a,b], R. Leonardi[a,b], G. Mantovani[a,b], M. Menichelli[a], A. Saha[a], A. Santocchia[a,b]

INFN Sezione di Pisa [a]**, Università di Pisa** [b]**, Scuola Normale Superiore di Pisa** [c]**, Pisa, Italy**
K. Androsov[a,32], P. Azzurri[a,15], G. Bagliesi[a], J. Bernardini[a], T. Boccali[a], R. Castaldi[a], M.A. Ciocci[a,32], R. Dell'Orso[a], S. Donato[a,c], G. Fedi, A. Giassi[a], M.T. Grippo[a,32], F. Ligabue[a,c], T. Lomtadze[a], L. Martini[a,b], A. Messineo[a,b], F. Palla[a], A. Rizzi[a,b], A. Savoy-Navarro[a,33], P. Spagnolo[a], R. Tenchini[a], G. Tonelli[a,b], A. Venturi[a], P.G. Verdini[a]

INFN Sezione di Roma [a]**, Università di Roma** [b]**, Roma, Italy**
L. Barone[a,b], F. Cavallari[a], G. D'imperio[a,b,15], D. Del Re[a,b,15], M. Diemoz[a], S. Gelli[a,b], C. Jorda[a], E. Longo[a,b], F. Margaroli[a,b], P. Meridiani[a], G. Organtini[a,b], R. Paramatti[a], F. Preiato[a,b], S. Rahatlou[a,b], C. Rovelli[a], F. Santanastasio[a,b]

INFN Sezione di Torino [a]**, Università di Torino** [b]**, Torino, Italy, Università del Piemonte Orientale** [c]**, Novara, Italy**
N. Amapane[a,b], R. Arcidiacono[a,c,15], S. Argiro[a,b], M. Arneodo[a,c], N. Bartosik[a], R. Bellan[a,b], C. Biino[a], N. Cartiglia[a], M. Costa[a,b], R. Covarelli[a,b], A. Degano[a,b], N. Demaria[a], L. Finco[a,b], B. Kiani[a,b], C. Mariotti[a], S. Maselli[a], E. Migliore[a,b], V. Monaco[a,b], E. Monteil[a,b], M.M. Obertino[a,b], L. Pacher[a,b], N. Pastrone[a], M. Pelliccioni[a], G.L. Pinna Angioni[a,b], F. Ravera[a,b], A. Romero[a,b], M. Ruspa[a,c], R. Sacchi[a,b], V. Sola[a], A. Solano[a,b], A. Staiano[a], P. Traczyk[a,b]

INFN Sezione di Trieste [a]**, Università di Trieste** [b]**, Trieste, Italy**
S. Belforte[a], V. Candelise[a,b], M. Casarsa[a], F. Cossutti[a], G. Della Ricca[a,b], C. La Licata[a,b], A. Schizzi[a,b], A. Zanetti[a]

Kangwon National University, Chunchon, Korea
S.K. Nam

Kyungpook National University, Daegu, Korea

D.H. Kim, G.N. Kim, M.S. Kim, D.J. Kong, S. Lee, S.W. Lee, Y.D. Oh, A. Sakharov, D.C. Son, Y.C. Yang

Chonbuk National University, Jeonju, Korea
J.A. Brochero Cifuentes, H. Kim, T.J. Kim[34]

Chonnam National University, Institute for Universe and Elementary Particles, Kwangju, Korea
S. Song

Korea University, Seoul, Korea
S. Cho, S. Choi, Y. Go, D. Gyun, B. Hong, Y. Jo, Y. Kim, B. Lee, K. Lee, K.S. Lee, S. Lee, J. Lim, S.K. Park, Y. Roh

Seoul National University, Seoul, Korea
H.D. Yoo

University of Seoul, Seoul, Korea
M. Choi, H. Kim, H. Kim, J.H. Kim, J.S.H. Lee, I.C. Park, G. Ryu, M.S. Ryu

Sungkyunkwan University, Suwon, Korea
Y. Choi, J. Goh, D. Kim, E. Kwon, J. Lee, I. Yu

Vilnius University, Vilnius, Lithuania
V. Dudenas, A. Juodagalvis, J. Vaitkus

National Centre for Particle Physics, Universiti Malaya, Kuala Lumpur, Malaysia
I. Ahmed, Z.A. Ibrahim, J.R. Komaragiri, M.A.B. Md Ali[35], F. Mohamad Idris[36], W.A.T. Wan Abdullah, M.N. Yusli, Z. Zolkapli

Centro de Investigacion y de Estudios Avanzados del IPN, Mexico City, Mexico
E. Casimiro Linares, H. Castilla-Valdez, E. De La Cruz-Burelo, I. Heredia-De La Cruz[37], A. Hernandez-Almada, R. Lopez-Fernandez, J. Mejia Guisao, A. Sanchez-Hernandez

Universidad Iberoamericana, Mexico City, Mexico
S. Carrillo Moreno, F. Vazquez Valencia

Benemerita Universidad Autonoma de Puebla, Puebla, Mexico
I. Pedraza, H.A. Salazar Ibarguen, C. Uribe Estrada

Universidad Autónoma de San Luis Potosí, San Luis Potosí, Mexico
A. Morelos Pineda

University of Auckland, Auckland, New Zealand
D. Krofcheck

University of Canterbury, Christchurch, New Zealand
P.H. Butler

National Centre for Physics, Quaid-I-Azam University, Islamabad, Pakistan
A. Ahmad, M. Ahmad, Q. Hassan, H.R. Hoorani, W.A. Khan, S. Qazi, M. Shoaib, M. Waqas

National Centre for Nuclear Research, Swierk, Poland
H. Bialkowska, M. Bluj, B. Boimska, T. Frueboes, M. Górski, M. Kazana, K. Nawrocki, K. Romanowska-Rybinska, M. Szleper, P. Zalewski

Institute of Experimental Physics, Faculty of Physics, University of Warsaw, Warsaw, Poland
G. Brona, K. Bunkowski, A. Byszuk[38], K. Doroba, A. Kalinowski, M. Konecki, J. Krolikowski, M. Misiura, M. Olszewski, M. Walczak

Laboratório de Instrumentação e Física Experimental de Partículas, Lisboa, Portugal
P. Bargassa, C. Beirão Da Cruz E Silva, A. Di Francesco, P. Faccioli, P.G. Ferreira Parracho, M. Gallinaro, J. Hollar, N. Leonardo, L. Lloret Iglesias, M.V. Nemallapudi, F. Nguyen, J. Rodrigues Antunes, J. Seixas, O. Toldaiev, D. Vadruccio, J. Varela, P. Vischia

Joint Institute for Nuclear Research, Dubna, Russia
S. Afanasiev, P. Bunin, M. Gavrilenko, I. Golutvin, I. Gorbunov, V. Karjavin, A. Lanev, A. Malakhov, V. Matveev[39,40], P. Moisenz, V. Palichik, V. Perelygin, M. Savina, S. Shmatov, S. Shulha, N. Skatchkov, V. Smirnov, N. Voytishin, A. Zarubin

Petersburg Nuclear Physics Institute, Gatchina (St. Petersburg), Russia
V. Golovtsov, Y. Ivanov, V. Kim[41], E. Kuznetsova[42], P. Levchenko, V. Murzin, V. Oreshkin, I. Smirnov, V. Sulimov, L. Uvarov, S. Vavilov, A. Vorobyev

Institute for Nuclear Research, Moscow, Russia
Yu. Andreev, A. Dermenev, S. Gninenko, N. Golubev, A. Karneyeu, M. Kirsanov, N. Krasnikov, A. Pashenkov, D. Tlisov, A. Toropin

Institute for Theoretical and Experimental Physics, Moscow, Russia
V. Epshteyn, V. Gavrilov, N. Lychkovskaya, V. Popov, I. Pozdnyakov, G. Safronov, A. Spiridonov, M. Toms, E. Vlasov, A. Zhokin

National Research Nuclear University 'Moscow Engineering Physics Institute' (MEPhI), Moscow, Russia
M. Chadeeva, R. Chistov, E. Popova, V. Rusinov, E. Tarkovskii

P.N. Lebedev Physical Institute, Moscow, Russia
V. Andreev, M. Azarkin[40], I. Dremin[40], M. Kirakosyan, A. Leonidov[40], G. Mesyats, S.V. Rusakov

Skobeltsyn Institute of Nuclear Physics, Lomonosov Moscow State University, Moscow, Russia
A. Baskakov, A. Belyaev, E. Boos, M. Dubinin[43], L. Dudko, A. Ershov, A. Gribushin, V. Klyukhin, O. Kodolova, I. Lokhtin, I. Miagkov, S. Obraztsov, S. Petrushanko, V. Savrin, A. Snigirev

State Research Center of Russian Federation, Institute for High Energy Physics, Protvino, Russia
I. Azhgirey, I. Bayshev, S. Bitioukov, V. Kachanov, A. Kalinin, D. Konstantinov, V. Krychkine, V. Petrov, R. Ryutin, A. Sobol, L. Tourtchanovitch, S. Troshin, N. Tyurin, A. Uzunian, A. Volkov

University of Belgrade, Faculty of Physics and Vinca Institute of Nuclear Sciences, Belgrade, Serbia
P. Adzic[44], P. Cirkovic, D. Devetak, J. Milosevic, V. Rekovic

Centro de Investigaciones Energéticas Medioambientales y Tecnológicas (CIEMAT), Madrid, Spain
J. Alcaraz Maestre, E. Calvo, M. Cerrada, M. Chamizo Llatas, N. Colino, B. De La Cruz, A. Delgado Peris, A. Escalante Del Valle, C. Fernandez Bedoya, J.P. Fernández Ramos, J. Flix, M.C. Fouz, P. Garcia-Abia, O. Gonzalez Lopez, S. Goy Lopez, J.M. Hernandez, M.I. Josa, E. Navarro De Martino, A. Pérez-Calero Yzquierdo, J. Puerta Pelayo, A. Quintario Olmeda, I. Redondo, L. Romero, M.S. Soares

Universidad Autónoma de Madrid, Madrid, Spain
J.F. de Trocóniz, M. Missiroli, D. Moran

Universidad de Oviedo, Oviedo, Spain
J. Cuevas, J. Fernandez Menendez, S. Folgueras, I. Gonzalez Caballero, E. Palencia Cortezon, J.M. Vizan Garcia

Instituto de Física de Cantabria (IFCA), CSIC-Universidad de Cantabria, Santander, Spain
I.J. Cabrillo, A. Calderon, J.R. Castiñeiras De Saa, E. Curras, M. Fernandez, J. Garcia-Ferrero, G. Gomez, A. Lopez Virto, J. Marco, R. Marco, C. Martinez Rivero, F. Matorras, J. Piedra Gomez, T. Rodrigo, A.Y. Rodríguez-Marrero, A. Ruiz-Jimeno, L. Scodellaro, N. Trevisani, I. Vila, R. Vilar Cortabitarte

CERN, European Organization for Nuclear Research, Geneva, Switzerland
D. Abbaneo, E. Auffray, G. Auzinger, M. Bachtis, P. Baillon, A.H. Ball, D. Barney, A. Benaglia, L. Benhabib, G.M. Berruti, P. Bloch, A. Bocci, A. Bonato, C. Botta, H. Breuker, T. Camporesi, R. Castello, M. Cepeda, G. Cerminara, M. D'Alfonso, D. d'Enterria, A. Dabrowski, V. Daponte, A. David, M. De Gruttola, F. De Guio, A. De Roeck, E. Di Marco[45], M. Dobson, M. Dordevic, B. Dorney, T. du Pree, D. Duggan, M. Dünser, N. Dupont, A. Elliott-Peisert, S. Fartoukh, G. Franzoni, J. Fulcher, W. Funk, D. Gigi, K. Gill, M. Girone, F. Glege, R. Guida, S. Gundacker, M. Guthoff, J. Hammer, P. Harris, J. Hegeman, V. Innocente, P. Janot, H. Kirschenmann, V. Knünz, M.J. Kortelainen, K. Kousouris, P. Lecoq, C. Lourenço, M.T. Lucchini, N. Magini, L. Malgeri, M. Mannelli, A. Martelli, L. Masetti, F. Meijers, S. Mersi, E. Meschi, F. Moortgat, S. Morovic, M. Mulders, H. Neugebauer, S. Orfanelli[46], L. Orsini, L. Pape, E. Perez, M. Peruzzi, A. Petrilli, G. Petrucciani, A. Pfeiffer, M. Pierini, D. Piparo, A. Racz, T. Reis, G. Rolandi[47], M. Rovere, M. Ruan, H. Sakulin, J.B. Sauvan, C. Schäfer, C. Schwick, M. Seidel, A. Sharma, P. Silva, M. Simon, P. Sphicas[48], J. Steggemann, M. Stoye, Y. Takahashi, D. Treille, A. Triossi, A. Tsirou, V. Veckalns[49], G.I. Veres[22], N. Wardle, H.K. Wöhri, A. Zagozdzinska[38], W.D. Zeuner

Paul Scherrer Institut, Villigen, Switzerland
W. Bertl, K. Deiters, W. Erdmann, R. Horisberger, Q. Ingram, H.C. Kaestli, D. Kotlinski, U. Langenegger, T. Rohe

Institute for Particle Physics, ETH Zurich, Zurich, Switzerland
F. Bachmair, L. Bäni, L. Bianchini, B. Casal, G. Dissertori, M. Dittmar, M. Donegà, P. Eller, C. Grab, C. Heidegger, D. Hits, J. Hoss, G. Kasieczka, P. Lecomte[†], W. Lustermann, B. Mangano, M. Marionneau, P. Martinez Ruiz del Arbol, M. Masciovecchio, M.T. Meinhard, D. Meister, F. Micheli, P. Musella, F. Nessi-Tedaldi, F. Pandolfi, J. Pata, F. Pauss, G. Perrin, L. Perrozzi, M. Quittnat, M. Rossini, M. Schönenberger, A. Starodumov[50], M. Takahashi, V.R. Tavolaro, K. Theofilatos, R. Wallny

Universität Zürich, Zurich, Switzerland
T.K. Aarrestad, C. Amsler[51], L. Caminada, M.F. Canelli, V. Chiochia, A. De Cosa, C. Galloni, A. Hinzmann, T. Hreus, B. Kilminster, C. Lange, J. Ngadiuba, D. Pinna, G. Rauco, P. Robmann, D. Salerno, Y. Yang

National Central University, Chung-Li, Taiwan
K.H. Chen, T.H. Doan, Sh. Jain, R. Khurana, M. Konyushikhin, C.M. Kuo, W. Lin, Y.J. Lu, A. Pozdnyakov, S.S. Yu

National Taiwan University (NTU), Taipei, Taiwan
Arun Kumar, P. Chang, Y.H. Chang, Y.W. Chang, Y. Chao, K.F. Chen, P.H. Chen, C. Dietz, F. Fiori, W.-S. Hou, Y. Hsiung, Y.F. Liu, R.-S. Lu, M. Miñano Moya, J.f. Tsai, Y.M. Tzeng

Chulalongkorn University, Faculty of Science, Department of Physics, Bangkok, Thailand
B. Asavapibhop, K. Kovitanggoon, G. Singh, N. Srimanobhas, N. Suwonjandee

Cukurova University, Adana, Turkey
A. Adiguzel, M.N. Bakirci[52], S. Cerci[53], S. Damarseckin, Z.S. Demiroglu, C. Dozen, I. Dumanoglu, E. Eskut, S. Girgis, G. Gokbulut, Y. Guler, E. Gurpinar, I. Hos, E.E. Kangal[54], A. Kayis Topaksu, G. Onengut[55], K. Ozdemir[56], A. Polatoz, C. Zorbilmez

Middle East Technical University, Physics Department, Ankara, Turkey
B. Bilin, S. Bilmis, B. Isildak[57], G. Karapinar[58], M. Yalvac, M. Zeyrek

Bogazici University, Istanbul, Turkey
E. Gülmez, M. Kaya[59], O. Kaya[60], E.A. Yetkin[61], T. Yetkin[62]

Istanbul Technical University, Istanbul, Turkey
A. Cakir, K. Cankocak, S. Sen[63]

Institute for Scintillation Materials of National Academy of Science of Ukraine, Kharkov, Ukraine
B. Grynyov

National Scientific Center, Kharkov Institute of Physics and Technology, Kharkov, Ukraine
L. Levchuk, P. Sorokin

University of Bristol, Bristol, United Kingdom
R. Aggleton, F. Ball, L. Beck, J.J. Brooke, D. Burns, E. Clement, D. Cussans, H. Flacher, J. Goldstein, M. Grimes, G.P. Heath, H.F. Heath, J. Jacob, L. Kreczko, C. Lucas, Z. Meng, D.M. Newbold[64], S. Paramesvaran, A. Poll, T. Sakuma, S. Seif El Nasr-storey, S. Senkin, D. Smith, V.J. Smith

Rutherford Appleton Laboratory, Didcot, United Kingdom
K.W. Bell, A. Belyaev[65], C. Brew, R.M. Brown, L. Calligaris, D. Cieri, D.J.A. Cockerill, J.A. Coughlan, K. Harder, S. Harper, E. Olaiya, D. Petyt, C.H. Shepherd-Themistocleous, A. Thea, I.R. Tomalin, T. Williams, S.D. Worm

Imperial College, London, United Kingdom
M. Baber, R. Bainbridge, O. Buchmuller, A. Bundock, D. Burton, S. Casasso, M. Citron, D. Colling, L. Corpe, P. Dauncey, G. Davies, A. De Wit, M. Della Negra, P. Dunne, A. Elwood, D. Futyan, Y. Haddad, G. Hall, G. Iles, R. Lane, R. Lucas[64], L. Lyons, A.-M. Magnan, S. Malik, L. Mastrolorenzo, J. Nash, A. Nikitenko[50], J. Pela, B. Penning, M. Pesaresi, D.M. Raymond, A. Richards, A. Rose, C. Seez, A. Tapper, K. Uchida, M. Vazquez Acosta[66], T. Virdee[15], S.C. Zenz

Brunel University, Uxbridge, United Kingdom
J.E. Cole, P.R. Hobson, A. Khan, P. Kyberd, D. Leslie, I.D. Reid, P. Symonds, L. Teodorescu, M. Turner

Baylor University, Waco, USA
A. Borzou, K. Call, J. Dittmann, K. Hatakeyama, H. Liu, N. Pastika

The University of Alabama, Tuscaloosa, USA
O. Charaf, S.I. Cooper, C. Henderson, P. Rumerio

Boston University, Boston, USA
D. Arcaro, A. Avetisyan, T. Bose, D. Gastler, D. Rankin, C. Richardson, J. Rohlf, L. Sulak, D. Zou

Brown University, Providence, USA
J. Alimena, G. Benelli, E. Berry, D. Cutts, A. Ferapontov, A. Garabedian, J. Hakala, U. Heintz, O. Jesus, E. Laird, G. Landsberg, Z. Mao, M. Narain, S. Piperov, S. Sagir, R. Syarif

University of California, Davis, Davis, USA
R. Breedon, G. Breto, M. Calderon De La Barca Sanchez, S. Chauhan, M. Chertok, J. Conway, R. Conway, P.T. Cox, R. Erbacher, C. Flores, G. Funk, M. Gardner, W. Ko, R. Lander, C. Mclean, M. Mulhearn, D. Pellett, J. Pilot, F. Ricci-Tam, S. Shalhout, J. Smith, M. Squires, D. Stolp, M. Tripathi, S. Wilbur, R. Yohay

University of California, Los Angeles, USA
R. Cousins, P. Everaerts, A. Florent, J. Hauser, M. Ignatenko, D. Saltzberg, E. Takasugi, V. Valuev, M. Weber

University of California, Riverside, Riverside, USA
K. Burt, R. Clare, J. Ellison, J.W. Gary, G. Hanson, J. Heilman, P. Jandir, E. Kennedy, F. Lacroix, O.R. Long, M. Malberti, M. Olmedo Negrete, M.I. Paneva, A. Shrinivas, H. Wei, S. Wimpenny, B. R. Yates

University of California, San Diego, La Jolla, USA
J.G. Branson, G.B. Cerati, S. Cittolin, R.T. D'Agnolo, M. Derdzinski, R. Gerosa, A. Holzner, R. Kelley, D. Klein, J. Letts, I. Macneill, D. Olivito, S. Padhi, M. Pieri, M. Sani, V. Sharma, S. Simon, M. Tadel, A. Vartak, S. Wasserbaech[67], C. Welke, J. Wood, F. Würthwein, A. Yagil, G. Zevi Della Porta

University of California, Santa Barbara, Santa Barbara, USA
J. Bradmiller-Feld, C. Campagnari, A. Dishaw, V. Dutta, K. Flowers, M. Franco Sevilla, P. Geffert, C. George, F. Golf, L. Gouskos, J. Gran, J. Incandela, N. Mccoll, S.D. Mullin, J. Richman, D. Stuart, I. Suarez, C. West, J. Yoo

California Institute of Technology, Pasadena, USA
D. Anderson, A. Apresyan, J. Bendavid, A. Bornheim, J. Bunn, Y. Chen, J. Duarte, A. Mott, H.B. Newman, C. Pena, M. Spiropulu, J.R. Vlimant, S. Xie, R.Y. Zhu

Carnegie Mellon University, Pittsburgh, USA
M.B. Andrews, V. Azzolini, A. Calamba, B. Carlson, T. Ferguson, M. Paulini, J. Russ, M. Sun, H. Vogel, I. Vorobiev

University of Colorado Boulder, Boulder, USA
J.P. Cumalat, W.T. Ford, F. Jensen, A. Johnson, M. Krohn, T. Mulholland, K. Stenson, S.R. Wagner

Cornell University, Ithaca, USA
J. Alexander, A. Chatterjee, J. Chaves, J. Chu, S. Dittmer, N. Eggert, N. Mirman, G. Nicolas Kaufman, J.R. Patterson, A. Rinkevicius, A. Ryd, L. Skinnari, L. Soffi, W. Sun, S.M. Tan, W.D. Teo, J. Thom, J. Thompson, J. Tucker, Y. Weng, P. Wittich

Fermi National Accelerator Laboratory, Batavia, USA
S. Abdullin, M. Albrow, G. Apollinari, S. Banerjee, L.A.T. Bauerdick, A. Beretvas, J. Berryhill, P.C. Bhat, G. Bolla, K. Burkett, J.N. Butler, H.W.K. Cheung, F. Chlebana, S. Cihangir, M. Cremonesi, V.D. Elvira, I. Fisk, J. Freeman, E. Gottschalk, L. Gray, D. Green, S. Grünendahl, O. Gutsche, D. Hare, R.M. Harris, S. Hasegawa, J. Hirschauer, Z. Hu, B. Jayatilaka, S. Jindariani, M. Johnson, U. Joshi, B. Klima, B. Kreis, S. Lammel, J. Lewis, J. Linacre, D. Lincoln, R. Lipton, T. Liu, R. Lopes De Sá, J. Lykken, K. Maeshima, J.M. Marraffino, S. Maruyama, D. Mason,

P. McBride, P. Merkel, S. Mrenna, S. Nahn, C. Newman-Holmes[†], V. O'Dell, K. Pedro, O. Prokofyev, G. Rakness, E. Sexton-Kennedy, A. Soha, W.J. Spalding, L. Spiegel, S. Stoynev, N. Strobbe, L. Taylor, S. Tkaczyk, N.V. Tran, L. Uplegger, E.W. Vaandering, C. Vernieri, M. Verzocchi, R. Vidal, M. Wang, H.A. Weber, A. Whitbeck

University of Florida, Gainesville, USA
D. Acosta, P. Avery, P. Bortignon, D. Bourilkov, A. Brinkerhoff, A. Carnes, M. Carver, D. Curry, S. Das, R.D. Field, I.K. Furic, J. Konigsberg, A. Korytov, K. Kotov, P. Ma, K. Matchev, H. Mei, P. Milenovic[68], G. Mitselmakher, D. Rank, R. Rossin, L. Shchutska, D. Sperka, N. Terentyev, L. Thomas, J. Wang, S. Wang, J. Yelton

Florida International University, Miami, USA
S. Linn, P. Markowitz, G. Martinez, J.L. Rodriguez

Florida State University, Tallahassee, USA
A. Ackert, J.R. Adams, T. Adams, A. Askew, S. Bein, J. Bochenek, B. Diamond, J. Haas, S. Hagopian, V. Hagopian, K.F. Johnson, A. Khatiwada, H. Prosper, A. Santra, M. Weinberg

Florida Institute of Technology, Melbourne, USA
M.M. Baarmand, V. Bhopatkar, S. Colafranceschi[69], M. Hohlmann, H. Kalakhety, D. Noonan, T. Roy, F. Yumiceva

University of Illinois at Chicago (UIC), Chicago, USA
M.R. Adams, L. Apanasevich, D. Berry, R.R. Betts, I. Bucinskaite, R. Cavanaugh, O. Evdokimov, L. Gauthier, C.E. Gerber, D.J. Hofman, P. Kurt, C. O'Brien, I.D. Sandoval Gonzalez, P. Turner, N. Varelas, Z. Wu, M. Zakaria, J. Zhang

The University of Iowa, Iowa City, USA
B. Bilki[70], W. Clarida, K. Dilsiz, S. Durgut, R.P. Gandrajula, M. Haytmyradov, V. Khristenko, J.-P. Merlo, H. Mermerkaya[71], A. Mestvirishvili, A. Moeller, J. Nachtman, H. Ogul, Y. Onel, F. Ozok[72], A. Penzo, C. Snyder, E. Tiras, J. Wetzel, K. Yi

Johns Hopkins University, Baltimore, USA
I. Anderson, B. Blumenfeld, A. Cocoros, N. Eminizer, D. Fehling, L. Feng, A.V. Gritsan, P. Maksimovic, M. Osherson, J. Roskes, U. Sarica, M. Swartz, M. Xiao, Y. Xin, C. You

The University of Kansas, Lawrence, USA
P. Baringer, A. Bean, C. Bruner, J. Castle, R.P. Kenny III, A. Kropivnitskaya, D. Majumder, M. Malek, W. Mcbrayer, M. Murray, S. Sanders, R. Stringer, Q. Wang

Kansas State University, Manhattan, USA
A. Ivanov, K. Kaadze, S. Khalil, M. Makouski, Y. Maravin, A. Mohammadi, L.K. Saini, N. Skhirtladze, S. Toda

Lawrence Livermore National Laboratory, Livermore, USA
D. Lange, F. Rebassoo, D. Wright

University of Maryland, College Park, USA
C. Anelli, A. Baden, O. Baron, A. Belloni, B. Calvert, S.C. Eno, C. Ferraioli, J.A. Gomez, N.J. Hadley, S. Jabeen, R.G. Kellogg, T. Kolberg, J. Kunkle, Y. Lu, A.C. Mignerey, Y.H. Shin, A. Skuja, M.B. Tonjes, S.C. Tonwar

Massachusetts Institute of Technology, Cambridge, USA
A. Apyan, R. Barbieri, A. Baty, R. Bi, K. Bierwagen, S. Brandt, W. Busza, I.A. Cali, Z. Demiragli, L. Di Matteo, G. Gomez Ceballos, M. Goncharov, D. Gulhan, D. Hsu, Y. Iiyama, G.M. Innocenti,

M. Klute, D. Kovalskyi, K. Krajczar, Y.S. Lai, Y.-J. Lee, A. Levin, P.D. Luckey, A.C. Marini, C. Mcginn, C. Mironov, S. Narayanan, X. Niu, C. Paus, C. Roland, G. Roland, J. Salfeld-Nebgen, G.S.F. Stephans, K. Sumorok, K. Tatar, M. Varma, D. Velicanu, J. Veverka, J. Wang, T.W. Wang, B. Wyslouch, M. Yang, V. Zhukova

University of Minnesota, Minneapolis, USA
A.C. Benvenuti, B. Dahmes, A. Evans, A. Finkel, A. Gude, P. Hansen, S. Kalafut, S.C. Kao, K. Klapoetke, Y. Kubota, Z. Lesko, J. Mans, S. Nourbakhsh, N. Ruckstuhl, R. Rusack, N. Tambe, J. Turkewitz

University of Mississippi, Oxford, USA
J.G. Acosta, S. Oliveros

University of Nebraska-Lincoln, Lincoln, USA
E. Avdeeva, R. Bartek, K. Bloom, S. Bose, D.R. Claes, A. Dominguez, C. Fangmeier, R. Gonzalez Suarez, R. Kamalieddin, D. Knowlton, I. Kravchenko, F. Meier, J. Monroy, F. Ratnikov, J.E. Siado, G.R. Snow, B. Stieger

State University of New York at Buffalo, Buffalo, USA
M. Alyari, J. Dolen, J. George, A. Godshalk, C. Harrington, I. Iashvili, J. Kaisen, A. Kharchilava, A. Kumar, A. Parker, S. Rappoccio, B. Roozbahani

Northeastern University, Boston, USA
G. Alverson, E. Barberis, D. Baumgartel, M. Chasco, A. Hortiangtham, A. Massironi, D.M. Morse, D. Nash, T. Orimoto, R. Teixeira De Lima, D. Trocino, R.-J. Wang, D. Wood, J. Zhang

Northwestern University, Evanston, USA
S. Bhattacharya, K.A. Hahn, A. Kubik, J.F. Low, N. Mucia, N. Odell, B. Pollack, M.H. Schmitt, K. Sung, M. Trovato, M. Velasco

University of Notre Dame, Notre Dame, USA
N. Dev, M. Hildreth, C. Jessop, D.J. Karmgard, N. Kellams, K. Lannon, N. Marinelli, F. Meng, C. Mueller, Y. Musienko[39], M. Planer, A. Reinsvold, R. Ruchti, N. Rupprecht, G. Smith, S. Taroni, N. Valls, M. Wayne, M. Wolf, A. Woodard

The Ohio State University, Columbus, USA
L. Antonelli, J. Brinson, B. Bylsma, L.S. Durkin, S. Flowers, A. Hart, C. Hill, R. Hughes, W. Ji, B. Liu, W. Luo, D. Puigh, M. Rodenburg, B.L. Winer, H.W. Wulsin

Princeton University, Princeton, USA
O. Driga, P. Elmer, J. Hardenbrook, P. Hebda, S.A. Koay, P. Lujan, D. Marlow, T. Medvedeva, M. Mooney, J. Olsen, C. Palmer, P. Piroué, D. Stickland, C. Tully, A. Zuranski

University of Puerto Rico, Mayaguez, USA
S. Malik

Purdue University, West Lafayette, USA
A. Barker, V.E. Barnes, D. Benedetti, L. Gutay, M.K. Jha, M. Jones, A.W. Jung, K. Jung, D.H. Miller, N. Neumeister, B.C. Radburn-Smith, X. Shi, J. Sun, A. Svyatkovskiy, F. Wang, W. Xie, L. Xu

Purdue University Calumet, Hammond, USA
N. Parashar, J. Stupak

Rice University, Houston, USA
A. Adair, B. Akgun, Z. Chen, K.M. Ecklund, F.J.M. Geurts, M. Guilbaud, W. Li, B. Michlin, M. Northup, B.P. Padley, R. Redjimi, J. Roberts, J. Rorie, Z. Tu, J. Zabel

University of Rochester, Rochester, USA
B. Betchart, A. Bodek, P. de Barbaro, R. Demina, Y.t. Duh, Y. Eshaq, T. Ferbel, M. Galanti, A. Garcia-Bellido, J. Han, O. Hindrichs, A. Khukhunaishvili, K.H. Lo, P. Tan, M. Verzetti

Rutgers, The State University of New Jersey, Piscataway, USA
J.P. Chou, E. Contreras-Campana, Y. Gershtein, T.A. Gómez Espinosa, E. Halkiadakis, M. Heindl, D. Hidas, E. Hughes, S. Kaplan, R. Kunnawalkam Elayavalli, S. Kyriacou, A. Lath, K. Nash, H. Saka, S. Salur, S. Schnetzer, D. Sheffield, S. Somalwar, R. Stone, S. Thomas, P. Thomassen, M. Walker

University of Tennessee, Knoxville, USA
M. Foerster, J. Heideman, G. Riley, K. Rose, S. Spanier, K. Thapa

Texas A&M University, College Station, USA
O. Bouhali[73], A. Castaneda Hernandez[73], A. Celik, M. Dalchenko, M. De Mattia, A. Delgado, S. Dildick, R. Eusebi, J. Gilmore, T. Huang, T. Kamon[74], V. Krutelyov, R. Mueller, I. Osipenkov, Y. Pakhotin, R. Patel, A. Perloff, L. Perniè, D. Rathjens, A. Rose, A. Safonov, A. Tatarinov, K.A. Ulmer

Texas Tech University, Lubbock, USA
N. Akchurin, C. Cowden, J. Damgov, C. Dragoiu, P.R. Dudero, J. Faulkner, S. Kunori, K. Lamichhane, S.W. Lee, T. Libeiro, S. Undleeb, I. Volobouev, Z. Wang

Vanderbilt University, Nashville, USA
E. Appelt, A.G. Delannoy, S. Greene, A. Gurrola, R. Janjam, W. Johns, C. Maguire, Y. Mao, A. Melo, H. Ni, P. Sheldon, S. Tuo, J. Velkovska, Q. Xu

University of Virginia, Charlottesville, USA
M.W. Arenton, P. Barria, B. Cox, B. Francis, J. Goodell, R. Hirosky, A. Ledovskoy, H. Li, C. Neu, T. Sinthuprasith, X. Sun, Y. Wang, E. Wolfe, F. Xia

Wayne State University, Detroit, USA
C. Clarke, R. Harr, P.E. Karchin, C. Kottachchi Kankanamge Don, P. Lamichhane, J. Sturdy

University of Wisconsin - Madison, Madison, WI, USA
D.A. Belknap, D. Carlsmith, S. Dasu, L. Dodd, S. Duric, B. Gomber, M. Grothe, M. Herndon, A. Hervé, P. Klabbers, A. Lanaro, A. Levine, K. Long, R. Loveless, A. Mohapatra, I. Ojalvo, T. Perry, G.A. Pierro, G. Polese, T. Ruggles, T. Sarangi, A. Savin, A. Sharma, N. Smith, W.H. Smith, D. Taylor, P. Verwilligen, N. Woods

†: Deceased
1: Also at Vienna University of Technology, Vienna, Austria
2: Also at State Key Laboratory of Nuclear Physics and Technology, Peking University, Beijing, China
3: Also at Institut Pluridisciplinaire Hubert Curien, Université de Strasbourg, Université de Haute Alsace Mulhouse, CNRS/IN2P3, Strasbourg, France
4: Also at Universidade Estadual de Campinas, Campinas, Brazil
5: Also at Centre National de la Recherche Scientifique (CNRS) - IN2P3, Paris, France
6: Also at Université Libre de Bruxelles, Bruxelles, Belgium
7: Also at Laboratoire Leprince-Ringuet, Ecole Polytechnique, IN2P3-CNRS, Palaiseau, France

8: Also at Joint Institute for Nuclear Research, Dubna, Russia

9: Also at Suez University, Suez, Egypt

10: Now at British University in Egypt, Cairo, Egypt

11: Also at Cairo University, Cairo, Egypt

12: Now at Helwan University, Cairo, Egypt

13: Now at Ain Shams University, Cairo, Egypt

14: Also at Université de Haute Alsace, Mulhouse, France

15: Also at CERN, European Organization for Nuclear Research, Geneva, Switzerland

16: Also at Skobeltsyn Institute of Nuclear Physics, Lomonosov Moscow State University, Moscow, Russia

17: Also at Tbilisi State University, Tbilisi, Georgia

18: Also at RWTH Aachen University, III. Physikalisches Institut A, Aachen, Germany

19: Also at University of Hamburg, Hamburg, Germany

20: Also at Brandenburg University of Technology, Cottbus, Germany

21: Also at Institute of Nuclear Research ATOMKI, Debrecen, Hungary

22: Also at MTA-ELTE Lendület CMS Particle and Nuclear Physics Group, Eötvös Loránd University, Budapest, Hungary

23: Also at University of Debrecen, Debrecen, Hungary

24: Also at Indian Institute of Science Education and Research, Bhopal, India

25: Also at University of Visva-Bharati, Santiniketan, India

26: Now at King Abdulaziz University, Jeddah, Saudi Arabia

27: Also at University of Ruhuna, Matara, Sri Lanka

28: Also at Isfahan University of Technology, Isfahan, Iran

29: Also at University of Tehran, Department of Engineering Science, Tehran, Iran

30: Also at Plasma Physics Research Center, Science and Research Branch, Islamic Azad University, Tehran, Iran

31: Also at Laboratori Nazionali di Legnaro dell'INFN, Legnaro, Italy

32: Also at Università degli Studi di Siena, Siena, Italy

33: Also at Purdue University, West Lafayette, USA

34: Now at Hanyang University, Seoul, Korea

35: Also at International Islamic University of Malaysia, Kuala Lumpur, Malaysia

36: Also at Malaysian Nuclear Agency, MOSTI, Kajang, Malaysia

37: Also at Consejo Nacional de Ciencia y Tecnología, Mexico city, Mexico

38: Also at Warsaw University of Technology, Institute of Electronic Systems, Warsaw, Poland

39: Also at Institute for Nuclear Research, Moscow, Russia

40: Now at National Research Nuclear University 'Moscow Engineering Physics Institute' (MEPhI), Moscow, Russia

41: Also at St. Petersburg State Polytechnical University, St. Petersburg, Russia

42: Also at University of Florida, Gainesville, USA

43: Also at California Institute of Technology, Pasadena, USA

44: Also at Faculty of Physics, University of Belgrade, Belgrade, Serbia

45: Also at INFN Sezione di Roma; Università di Roma, Roma, Italy

46: Also at National Technical University of Athens, Athens, Greece

47: Also at Scuola Normale e Sezione dell'INFN, Pisa, Italy

48: Also at National and Kapodistrian University of Athens, Athens, Greece

49: Also at Riga Technical University, Riga, Latvia

50: Also at Institute for Theoretical and Experimental Physics, Moscow, Russia

51: Also at Albert Einstein Center for Fundamental Physics, Bern, Switzerland

52: Also at Gaziosmanpasa University, Tokat, Turkey

53: Also at Adiyaman University, Adiyaman, Turkey
54: Also at Mersin University, Mersin, Turkey
55: Also at Cag University, Mersin, Turkey
56: Also at Piri Reis University, Istanbul, Turkey
57: Also at Ozyegin University, Istanbul, Turkey
58: Also at Izmir Institute of Technology, Izmir, Turkey
59: Also at Marmara University, Istanbul, Turkey
60: Also at Kafkas University, Kars, Turkey
61: Also at Istanbul Bilgi University, Istanbul, Turkey
62: Also at Yildiz Technical University, Istanbul, Turkey
63: Also at Hacettepe University, Ankara, Turkey
64: Also at Rutherford Appleton Laboratory, Didcot, United Kingdom
65: Also at School of Physics and Astronomy, University of Southampton, Southampton, United Kingdom
66: Also at Instituto de Astrofísica de Canarias, La Laguna, Spain
67: Also at Utah Valley University, Orem, USA
68: Also at University of Belgrade, Faculty of Physics and Vinca Institute of Nuclear Sciences, Belgrade, Serbia
69: Also at Facoltà Ingegneria, Università di Roma, Roma, Italy
70: Also at Argonne National Laboratory, Argonne, USA
71: Also at Erzincan University, Erzincan, Turkey
72: Also at Mimar Sinan University, Istanbul, Istanbul, Turkey
73: Also at Texas A&M University at Qatar, Doha, Qatar
74: Also at Kyungpook National University, Daegu, Korea